

---

# Phylogenetic relationships of spatangoid sea urchins (Echinoidea): taxon sampling density and congruence between morphological and molecular estimates

BRUCE STOCKLEY, ANDREW B. SMITH, TIM LITTLEWOOD, HARILAOS A. LESSIOS & JACQUELINE A. MACKENZIE-DODDS

---

Accepted: 13 April 2005  
doi:10.1111/j.1463-6409.2005.00201.x

Stockley, B., Smith, A. B., Littlewood T., Lessios H. A. & MacKenzie-Dodds J. A. (2005). Phylogenetic relationships of spatangoid sea urchins (Echinoidea): taxon sampling density and congruence between morphological and molecular estimates. — *Zoologica Scripta*, \*\*, \*\*\*-\*\*\*.

A phylogeny for 21 species of spatangoid sea urchins is constructed using data from three genes and results compared with morphology-based phylogenies derived for the same taxa and for a much larger sample of 88 Recent and fossil taxa. Different data sets and methods of analysis generate different phylogenetic hypotheses, although congruence tests show that all molecular approaches produce trees that are congruent with each other. By contrast, the trees generated from morphological data differ significantly according to taxon sampling density and only those with dense sampling (after *a posteriori* weighting) are congruent with molecular estimates. With limited taxon sampling, secondary reversals in deep-water taxa are interpreted as plesiomorphies, pulling them to a basal position. The addition of fossil taxa with their unique character combinations reveals hidden homoplasy and generates a phylogeny that is compatible with molecular estimates. As homoplasy levels were found to be broadly similar across different anatomical structures in the echinoid test, no one suite of morphological characters can be considered to provide more reliable phylogenetic information. Some traditional groupings are supported, including the grouping of Loveniidae, Brissidae and Spatangidae within the Micrasterina, but the Asterostomatidae is shown to be polyphyletic with members scattered amongst at least five different clades. As these are mostly deep-sea taxa, this finding implies multiple independent invasions into the deep sea.

Bruce Stockley, Andrew Smith, Tim Littlewood, Jacqueline A. MacKenzie-Dodds, The Natural History Museum, Cromwell Road, London SW67 5BD, UK. E-mail: a.smith@nhm.ac.uk  
Harilaos Lessios, Smithsonian Tropical Research Institute, Balboa, Panama. E-mail: Lessiosb@stri.org

## Introduction

The combined use of morphological and molecular data to investigate phylogenetic relationships is now standard practice, with data from the two sources usually being kept separate at least initially for comparative purposes (De Queiroz *et al.* 1995). In many cases the two data sets provide compatible (though rarely identical) topologies, and the two can safely be combined. However, data sets drawn from multiple genes or from morphology and molecular sources are sometimes so different that there is no justification for treating them as suboptimal estimates of the same underlying topology (see Larson 1994; Farris *et al.* 1994; Cunningham 1997). A decision has then to be made as to which is more likely to be in error. The causes of significant mismatch between independent data sets are thus usually attributed to biases inherent in the data rather than to inadequate sampling (either of characters or taxa).

A number of parallel molecular and morphological studies of echinoderms have been carried out, focusing on the relationships of the five classes (e.g. Littlewood *et al.* 1997; Janies 2001; Smith *et al.* 2004), or on relationships within the individual classes (e.g. Smith *et al.* 1995a,b; Littlewood & Smith 1995; Lafay *et al.* 1995; Kerr & Kim 2001; Jeffery *et al.* 2003). In all these studies the limiting factor has been the number of taxa available for molecular sampling. Every taxon available for gene sequencing can usually also be included in a morphological analysis, but the converse is not true. Furthermore, in groups such as sea urchins, much denser sampling of morphology can be obtained if the fossil record is taken into account. Here we provide an example where the addition of fossil taxa and denser sampling across a clade help resolve an apparent conflict between morphological and molecular trees.

### Previous work on spatangoid phylogeny

The Spatangoida, or heart urchins, are the most diverse of all the extant orders of sea urchin. They make up a quarter of all living urchin species, and have a rich fossil record, extending back over 145 million years (Villier *et al.* 2004). They are to be found in all the major oceans of the world, and vary in their geographical distribution from highly localized to highly cosmopolitan. Spatangoids are predominantly infaunal, and they are able to live in virtually all types of marine sediment (Ghiold 1988; Ghiold & Hoffman 1989). However, some spatangoids have adopted an epifaunal life style, particularly those species living in the deep sea. Recorded depths of spatangoids (Mortensen 1950, 1951) range from the sublittoral zone to the abyssal depths (> 6000 m), and they are one of a small number of echinoid groups to have successfully colonized the deepest of marine waters.

Despite their diversity and importance, there has been no modern analysis of how extant spatangoids are related, and our classification of the group still relies very heavily on the morphological framework established by Mortensen (1950, 1951). Mortensen used the term Spatangoida to include a diverse range of forms, distinguishing three major groups on the basis of their plastron structure. Subsequently, Durham & Melville (1957) restricted the Spatangoida to include just those forms with an amphisternous plastron, and we, like all subsequent workers, follow this more restricted usage.

Mortensen (1950, 1951) gave a comprehensive review of earlier work and revised all living species, dividing amphisternous forms into eight families (Table 1). His family-level taxonomy relied almost entirely upon just two features, the structure of the apical disc and the presence or absence of specific types of fasciole (bands of specialized ciliated spines that play a critical role in allowing spatangoids to live infaunally, see Lawrence

1987; Smith & Stockley 2005). Although Mortensen did not group these families into any higher taxonomic arrangement, he did regard the Paleopneustidae (under the incorrect spelling Palaeopneustidae) as the most primitive of extant families. This was because Paleopneustidae lack fascioles, an attribute shared with the stratigraphically oldest and most primitive of fossil spatangoids, the Toxasteridae. The great majority of extant deep-sea spatangoids fell into Mortensen's Paleopneustidae.

Fischer (1966) followed Mortensen's scheme closely, dividing spatangoids into 11 families (Table 1). These he grouped into four suborders: the Toxasterina, Hemiasterina, Micrasterina, and Asterostomatina (the latter being equivalent to Mortensen's Paleopneustidae and encompassing all extant forms lacking fascioles). Like Mortensen, Fischer based his classification on the same two characters of apical disc structure and fasciole distribution.

Since Fischer's (1966) study, there has been little new material published on the higher taxonomy of spatangoids. Chesher (1968) started to develop a more considered approach to the use of fascioles in spatangoid classification. He realized that the precise path followed by individual fascioles across the plating of the test was both highly conserved within species and phylogenetically informative. He noted that *Paleopneustes* and Pericosmidae had identical fasciole bands and that *Paleopneustes* was distinct from the majority of taxa placed by Fischer (1966) in the Asterostomatina. This led him to synonymize the Paleopneustidae and Pericosmidae and to transfer the majority of genera that Mortensen included in the Paleopneustidae to the Asterostomatidae.

Markov & Solovjev (2001) developed Chesher's work further by recognizing that the latero-anal fasciole of schizasterid spatangoids and the marginal fasciole of paleopneustids were homologous, and used this to unite the two families into a clade named Paleopneustoidea. Most recently, a wide-ranging review of fascioles and their homology has been undertaken (Smith & Stockley 2005) covering the great majority of fasciole-bearing spatangoid genera. This refined homology concepts amongst spatangoids and recognized several potential clades based on fasciole architecture.

One additional family, the Somaliasteridae, has been transferred from the Holasteroidea into the Spatangoida by Jeffery (1999). She argued that this peculiar group of four extinct genera were spatangoids with specialized plastron plating.

One of the major problems that has hampered spatangoid systematics is the emphasis that has traditionally been placed on fascioles (Neraudeau *et al.* 1998; Villier *et al.* 2004; Smith & Stockley 2005). The absence of fascioles may be primitive, but could, as Mortensen (1950) and Fischer (1966) acknowledged, also represent a secondary loss, for example with a switch from an infaunal to an epibenthic mode of life. It is therefore imperative that classifications and phylogenetic hypotheses of spatangoids are constructed from all available data. The recent paper by

**Table 1** Classification of the Spatangoida by Mortensen (1950) and Fischer (1966).

Mortensen	Fischer
Order Spatangoida	Order Spatangoida
Family Toxasteridae	Suborder Toxasterina
Family Hemiasteridae	Family Toxasteridae
Family Palaeostomatidae	Suborder Hemiasterina
Family Pericosmidae	Family Hemiasteridae
Family Schizasteridae	Family Palaeostomatidae
Family Aeropsidae	Family Pericosmidae
Family Micrasteridae	Family Schizasteridae
Family Brissidae	Family Aeropsidae
Family Spatangidae	Suborder Micrasterina
Family Loveniidae	Family Micrasteridae
Family Palaeopneustidae	Family Brissidae
	Family Spatangidae
	Family Loveniidae
	Suborder Asterostomatina
	Family Asterostomatidae

Villier *et al.* (2004) has started this process by compiling a large database of morphological characters for the early Cretaceous genera of Spatangoida and subjecting it to a rigorous cladistic analysis. Their study examined a broad cross-section of primitive taxa and found support for Fischer's Micrasterina and Hemiasterina groupings; however, they did not include taxa younger than mid-Cretaceous.

In this paper we provide a dual molecular and morphological analysis of spatangoid phylogeny to generate a phylogeny and revised taxonomy for the entire group, investigate how many independent lineages are living in the deep sea, and explore the value of wider taxon sampling.

## Materials and methods

### Taxa and outgroups

Twenty-one species of Spatangoida, representing 18 genera, and five of Mortensen's eight extant families (Table 2), form the core of this study. Three genera — *Brisaster* (Schizasteridae), *Metalia* (Brissidae), and *Spatangus* (Spatangidae) — were each represented by two species so that regions of highly variable gene sequence at the congeneric level could be identified and removed. Morphological data were collected for these 21 species as well as for a much larger sample of taxa comprising 88 genera, both Recent and fossil. In almost all cases type species were selected as exemplars for the genera. Information on these taxa is available in Smith (2004).

As outgroup for the morphological analyses we used *Toxaster retusus*, one of the stratigraphically earliest fossils and one that

has traditionally been considered as one of the most primitive (Mortensen 1950, 1951; Fischer 1966; Villier *et al.* 2004). For rooting molecular data we used three outgroups: *Plexechinus*, *Echinoneus* and *Conolampas*. *Plexechinus* is a member of the Holasteroidea, the closest extant sister group to spatangoids, and split from Spatangoida approximately 140 million years ago. *Conolampas* is a representative of the Cassiduloidea and diverged from spatangoids about 180 million years ago, while *Echinoneus* is considered to be the most primitive living irregular echinoid (Smith & Wright 1999).

### Morphological methods

All morphological characters used in this study were defined by direct examination of specimens, using a low power light microscope. Seventy-nine characters relating to skeletal architecture and tuberculation were scored. The full list of characters, with descriptions of character states and coding, is given in Appendix 1. Data on pedicellariae morphology were also collected but quickly abandoned as they proved to be highly variable amongst extant species and unavailable from fossil taxa.

All but three of the characters (6, 46, 77) were treated as unordered. Three characters, relating to the development of the frontal groove (depth of groove adapically, at ambitus and adorally; characters 8–10 in Appendix 1) were each given a weight of 0.333 so as to give the character 'development of frontal groove' the same weight as other test features. All other characters were given equal weight.

**Table 2** Spatangoid taxa sequenced with EMBL/GenBank database accession numbers given where sequence data was produced.

Genus	Species	Author	28S	16S	COI
<i>Abatus</i>	<i>cavernosus</i>	Philippi (1845)	AJ639776	AJ639803	AJ639904
<i>Agassizia</i>	<i>scrobiculata</i>	Valenciennes (1846)	AJ639779	AJ639802	
<i>Allobrissus</i>	<i>agassizii</i>	Doderlein (1885)	AJ639799	AJ639823	AJ639920
<i>Amphipneustes</i>	<i>lorioli</i>	Koehler (1901)	AJ639780	AJ639804	AJ639905
<i>Archaeopneustes</i>	<i>hystrix</i>	A. Agassiz (1880)	AJ639785	AJ639809	AJ639909
<i>Brisaster</i>	<i>fragilis</i>	Duben & Koren (1844)	AJ639781	AJ639805	AJ639906
<i>Brisaster</i>	<i>latifrons</i>	A. Agassiz (1898)	AJ639782	AJ639806	
<i>Brissopsis</i>	<i>atlantica</i>	Mortensen (1907)	AJ639794	AJ639818	AJ639917
<i>Brissus</i>	<i>obessus</i>	Verrill (1867)	AJ639797	AJ639821	
<i>Conolampas</i>	<i>sigsbei</i>	A. Agassiz (1878)	AJ639777	AJ639800	AJ639902
<i>Echinocardium</i>	<i>laevigaster</i>	A. Agassiz (1869)	AJ639789	AJ639813	AJ639913
<i>Echinoneus</i>	<i>cyclostomus</i>	Leske (1778)	AJ639778	AJ639801	AJ639903
<i>Linopneustes</i>	<i>longispinus</i>	A. Agassiz (1878)	AJ639795	AJ639819	AJ639918
<i>Lovenia</i>	<i>cordiformis</i>	A. Agassiz (1872)	AJ639790	AJ639814	AJ639914
<i>Meoma</i>	<i>ventricosa</i>	Lamarck (1816)	AJ639796	AJ639820	AJ639919
<i>Metalia</i>	<i>spatagus</i>	Linnaeus (1758)	AJ639791	AJ639815	AJ639915
<i>Metalia</i>	<i>nobilis</i>	Verrill (1867–71)	AJ639792	AJ639816	
<i>Palaeopneustes</i>	<i>cristatus</i>	A. Agassiz (1873)	AJ639784	AJ639808	AJ639908
<i>Paramaretia</i>	<i>multituberculata</i>	Mortensen (1950)	AJ639788	AJ639812	AJ639912
<i>Paraster</i>	<i>doederleni</i>	Chesher (1972)	AJ639783	AJ639807	AJ639907
<i>Plagiobrissus</i>	<i>grandis</i>	Gmelin (1788)	AJ639793	AJ639817	AJ639916
<i>Plexechinus</i>	<i>planus</i>	Mironov (1978)	AY957469	AY957467	
<i>Spatangus</i>	<i>raschi</i>	Loven (1869)	AJ639787	AJ639811	AJ639911
<i>Spatangus</i>	<i>multispinus</i>	Mortensen (1925)	AJ639786	AJ639810	AJ639910

**Table 3** Character weighting scheme (*a posteriori*, based on maximum rescaled consistency index).

---

1 (0.071429), 2 (0.134615), 3 (0.277778), 4 (0.088319), 5 (1.00000), 6 (0.622222), 7 (0.222222), 8 (0.055000), 9 (0.031008), 10 (0.057143), 11 (0.104072), 12 (0.134615), 13 (0.125000), 14 (0.000000), 15 (0.074074), 16 (0.080808), 17 (0.060185), 18 (1.000000), 19 (1.000000), 20 (0.064327), 21 (0.123932), 22 (1.000000), 23 (0.123377), 24 (0.107143), 25 (1.000000), 26 (0.000000), 27 (0.178571), 28 (0.047059), 29 (0.250000), 30 (0.078189), 31 (0.166667), 32 (0.107143), 33 (0.071111), 34 (0.119555), 35 (0.000000), 36 (0.166667), 37 (1.000000), 38 (1.000000), 39 (0.312500), 40 (1.000000), 41 (0.368421), 42 (0.315789), 43 (0.092593), 44 (0.154286), 45 (0.083810), 46 (0.103955), 47 (0.000000), 48 (0.000000), 49 (0.084615), 50 (0.333333), 51 (0.075000), 52 (1.000000), 53 (1.000000), 54 (0.485294), 55 (0.303030), 56 (1.000000), 57 (1.000000), 58 (0.105882), 59 (0.066667), 60 (1.000000), 61 (0.051383), 62 (0.070312), 63 (0.470588), 64 (1.000000), 65 (0.166667), 66 (0.146667), 67 (0.000000), 68 (0.244444), 69 (0.062500), 70 (0.054545), 71 (0.333333), 72 (1.000000), 73 (0.000000), 74 (0.046667), 75 (0.142857), 76 (1.000000), 77 (0.266667), 78 (0.238095), 79 (0.110672)
---

---

Phylogenetic analysis was carried out using the Macintosh version of PAUP\* 4.0b10 (Altevec) (Swofford 2002). As the large number of taxa precluded a branch and bound or exhaustive search of the matrix, we used a heuristic search method, with random additional replicates and TBR branch swapping. Bootstrapping was carried out to test node support and Bremer support was also calculated (Bremer 1994).

Two analyses were run: one using the full set of 88 taxa (full dataset) and the other including just those genera for which molecular data were available, plus an outgroup (19 genera — the core dataset). For the core dataset, 2000 random addition replicates were run and bootstrapping was carried out with 1000 replicates. Heuristic searches of the full dataset of 88 taxa proved to be much more time-consuming and just 25 random replicates were run. This generated multiple equally parsimonious trees and so the characters were then reweighted by the maximum rescaled consistency index of the initial trees (weightings used are given in Table 3) and the analysis rerun with 1000 random addition replicates.

#### **Molecular methods**

**Gene selection.** Three genes were selected for analysis: the mitochondrial 16S rRNA (16S), cytochrome c oxidase subunit 1 (COI) and nuclear 28S rRNA (28S) genes. These were chosen because they had been used successfully in earlier studies (Littlewood & Smith 1995; Jeffery *et al.* 2003) and were known to encompass the range of rates of evolution needed to resolve divergences over the past 150 million years. Approximately 630 base pairs from the 3' end of the 16S gene, 800 base pairs from the 5' end of the COI gene and 1250 base pairs from the 5' end of the 28S gene were amplified.

#### **DNA extraction, amplification, sequencing and alignment**

Specimens were freshly collected and either frozen or fixed in absolute ethanol prior to tissue extraction. Several micrograms of tissue were excised from specimens. Gonadal material was used preferentially, but, where unavailable, tissue was obtained from phyllode tube feet, primary spine muscle, or peristomial membrane. Tissue from ethanol-preserved specimens was washed in distilled water prior to DNA extraction, whilst tissue from frozen specimens was simply defrosted. Whole genomic DNA was extracted using a DNeasy tissue kit (Qiagen), according

to the manufacturer's protocol. In cases where subsequent PCR amplification failed, this whole genomic DNA was further purified by using a QIAquick PCR purification column (Qiagen) according to the manufacturer's protocol.

Amplifications of 16S and 28S fragments were performed using the HotStarTaq PCR amplification kit (Qiagen), with 20 µL reaction volumes. Each reaction tube contained 1–5 µL (approx 20 ng) of genomic DNA extract, 1 U Taq polymerase, 2.5 mM MgCl<sub>2</sub>, 1X PCR buffer (proprietary, Qiagen), 1X 'Q' solution (proprietary, Qiagen), and 10 picomoles of each external PCR primer (Table 4). PCR conditions used were: 15-minute denaturation at 95 °C; 35 cycles of 50 s at 94 °C, 50 s at 52 °C, 60 s at 72 °C, then held at 4 °C until used.

Amplifications of COI fragments were performed using the BioTaq DNA polymerase kit (Bioline), with 20 µL reaction volumes. Each reaction tube contained; 5 µL (approx 40 ng) of genomic DNA extract, 2.5 U Taq polymerase, 2.5 mM MgCl<sub>2</sub> (1X PCR buffer (containing 8 mM (NH<sub>4</sub>)<sub>2</sub>SO<sub>4</sub>, 33.5 mM Tris-HCl (pH 8.8 at 25 °C), 0.005% Tween-20), 1X 'BioEnhance' solution (Proprietary, BioLine), and 10 picomoles of each external PCR primer (Table 4). PCR conditions used were 4-minute denaturation at 94 °C, 35 cycles of 50 s at 94 °C, 30 s at 52 °C, 60 s at 72 °C, then held at 72 °C for 5 min, then held at 4 °C until used.

PCR products were purified with Qiagen QIAquick columns, and cycle-sequenced directly using ABI Big-Dye chemistry, according to manufacturers' protocols. The sequencing reactions were purified using ethanol precipitation, and run on an ABI Prism 377 autosequencer. 16S fragments were sequenced using only internal primers, but the 28S fragments were sequenced in several overlapping subsections using a variety of internal primers listed in Table 4.

Sequence data were obtained for both forward and reverse reads of each fragment, to check base-pair reads. An initial pairwise alignment was made using MacClade (Maddison & Maddison 2001) followed by alignment of sequences by eye. Areas of high variability, and with strong within-genus variability in particular for which no reliable alignment could be made, were excluded from further data analysis. Two short regions in the 16S rRNA gene could be aligned unambiguously for just the spatangoid taxa but not with outgroups included. Rather than omitting these regions and thereby throwing away potentially phylogenetically

**Table 4** Primers used for PCR amplification and sequencing of fragments of 28S, 16S, and COI genes.

Primer Name	Gene amplified	Species amplified	Primer sequence 5'- to 3'
28S23L	LSU external	All	GAC CTC AGA TCG GAC GAG AC
28S278L	LSU internal	All	CAA GGC TAA ATA CTG GCA CGA
28S866L	LSU internal	All	GTC TCC CCG GCG TTC ACT
28S1344R	LSU external	All	CAA GGC CTC TAA TCA TTC GCT
28S872R	LSU internal	All	TGA GTA CAG TGA ACG CCG
28S278R	LSU internal	All	TCG TGC CAG TAT TTA GCC TTG
28Sbf392L	LSU internal	<i>Brisaster fragilis</i>	AAG AAG CAA ACG AGC AGG AC
28Spd582L	LSU internal	<i>Paraster dodderleini</i>	GAC TAA TAG CGC GCA CGA C
28Smv754R	LSU internal	<i>Meoma ventricosa</i>	CGT CCC TCA GCG ACC ACT
28Slc727R	LSU internal	<i>Lovenia cordiformis</i>	AGT GAA CGC CGG GGA GAC T
28S708V3R	LSU internal	<i>Allobrissus agassizii</i>	GGC TC(AG) CGT CCC TTC CTC
—	—	<i>Archaeopneustes hystrix</i>	—
—	—	<i>Brisaster fragilis</i>	—
—	—	<i>Echinocardium laevigaster</i>	—
—	—	<i>Linopneustes longispinus</i>	—
—	—	<i>Spatangus rashi</i>	—
28Sms699R	LSU internal	<i>Metalia spatagus</i>	TAA ACG CCG GGG AGA CCT
28Spm680R	LSU internal	<i>Paramaretia multituberculata</i>	GAG GCG CAG CCC CAG ATG
28Sal649R	LSU internal	<i>Amphipneustes lorioli</i>	GTC CCT TCC TCG GCA GCT C
28Ssm571R	LSU internal	<i>Spatangus multispinus</i>	CTG CGC GCT ATT AGT CTT CC
28Spd500R	LSU internal	<i>Paraster dodderleini</i>	GAC CGG GTG ACG GAG ATA C
28Sms436R	LSU internal	<i>Metalia spatagus</i>	CGA GGA GCC TGA AGA CGG AG
16Sech5	SSU external	All	CGC CTG TTT ACC AAA AAC AT
16Sech3	SSU external	All	TCG TAG ATA GAA ACT GAC CTG
COIe5	COI external	All	GC(CT) TGA GC(AT) GGC ATG GTA GG
COIe3	COI external	All	GCT CGT GT(AG) TCT AC(AG) TCC AT
COIRint	COI internal	<i>Abatus cavernosus</i>	AAA GAG ATT CCT GG(AGT) GCT CG
—	—	<i>Allobrissus agassizii</i>	—
—	—	<i>Archaeopneustes hystrix</i>	—
—	—	<i>Brisaster fragilis</i>	—
—	—	<i>Echinocardium laevigaster</i>	—
—	—	<i>Linopneustes longispinus</i>	—
—	—	<i>Lovenia cordiformis</i>	—
—	—	<i>Meoma ventricosa</i>	—
—	—	<i>Paraster dodderleini</i>	—
—	—	<i>Palaeopneustes cristatus</i>	—
—	—	<i>Plagiobrissus grandis</i>	—
—	—	<i>Paramaretia multituberculata</i>	—
COIRintV2	COI internal	<i>Abatus cavernosus</i>	CGG TCA AA(AG) GAA ATT CC(AG) GG
—	—	<i>Allobrissus agassizii</i>	—
—	—	<i>Brissopsis elongata</i>	—
—	—	<i>Metalia sternalis</i>	—
—	—	<i>Paraster dodderleini</i>	—
COILint	COI internal	<i>Abatus cavernosus</i>	GC(ACT) TCA TCA ATT CTA GCC TCT AT
—	—	<i>Brissopsis elongata</i>	—
—	—	<i>Brisaster fragilis</i>	—
—	—	<i>Echinocardium laevigaster</i>	—
—	—	<i>Spatangus multispinus</i>	—
COILintV2	COI internal	<i>Allobrissus agassizii</i>	AA(AC) ATA GC(AC) CAC GCA GGA GG
—	—	<i>Archaeopneustes hystrix</i>	—
—	—	<i>Brisaster fragilis</i>	—
—	—	<i>Lovenia cordiformis</i>	—
—	—	<i>Meoma ventricosa</i>	—
—	—	<i>Plagiobrissus grandis</i>	—

informative sites, these regions were included but with the outgroup taxa scored as unknown (?). In total, out of 2225 aligned base pairs, 465 were phylogenetically informative.

All sequences are lodged with EMBO, under accession numbers listed in Table 2.

#### *Analysis methods used*

Analysis using the optimality criterion of maximum parsimony (MP) was performed using the same version of PAUP\* as used in the morphological methods. Gaps were treated as missing data (because there were so few, treating gaps as a new (5th)

state made no difference to the resultant trees). All character state transformations were treated as of equal weight. Data sets were bootstrapped with 1000 replicates.

Modeltest v. 3.06 for Macintosh (Posada & Crandall 1998) was used to analyse each data set and produce an appropriate model of genetic evolution for maximum likelihood (ML) and Bayes analysis. Two different models were used: for ML we used the simpler HKY85 model with transition-transversion ratio and base frequencies estimated empirically, for Bayes analyses we used the GTR + G + I model (rates set to gamma, with six substitution types). Bayesian inference analyses were conducted using a separate GTR + G + I model for each data partition independently, and also for the combined three-gene analysis, thus allowing separate estimates for each model parameter per data set.

ML analysis was performed using the same version of PAUP\* as the MP analysis. The maximum number of trees in memory was not limited. Data sets were bootstrapped with 150 replicates.

Bayes analysis was performed using both the Macintosh and the Unix versions of MrBayes (Huelsenbeck & Ronquist 2003). The number of generations permitted was 1 000 000 with four chains, and a burn in of 5000. The consensus tree was constructed from the nonburn in trees, and was a 50% majority rule tree.

#### Data congruence tests

To investigate the appropriateness of combining the gene data sets, the Partition Homogeneity (Farris *et al.* 1994) option in PAUP\* was executed.

A Templeton test of data heterogeneity (described by Larson 1994; and implemented in PAUP\* under the 'describe trees'

option) was performed on the various trees that were obtained from morphological and molecular data sets under the different analytical procedures, to explore whether they could be considered suboptimal estimates of the same underlying topology. For comparison, the tree generated from morphological data and based on 88 taxa was pruned so that it contained only those taxa common to the molecular data sets being compared.

## Results

### Morphological results

Parsimony analysis of the morphological data for the 18 core genera plus outgroup produced two equally most parsimonious trees, length (TL) 174.61, a retention index (RI) of 0.58, and a consistency index (CI) of 0.51 (Fig. 1A). However, relatively few nodes were supported by bootstrap values greater than 50%. Analysis of the set of 88 taxa without weighting found 454 trees (TL 525.11, RI = 0.66, CI = 0.21). The main area of uncertainty was created by a large polytomy in the Schizasteridae. After reweighting and rerunning the analysis, 57 trees (TL = 69.31, RI = 0.81, CI = 0.32) were found. A strict consensus of these trees is shown in Fig. 2. Many traditionally recognized groupings are supported in this tree, but the genera Fischer (1966) placed in his Asterostomatidae are widely scattered across the topology. For comparison, a stripped version of this topology, showing the relationships of the 18 genera for which we have molecular data is shown in Fig. 1B.

Although some of the more terminal parts of the topologies estimated from the full dataset and the reduced dataset are identical there are striking differences in the position of *Amphipneustes*, *Archaeopneustes* and *Brissopsis* in the two estimates.

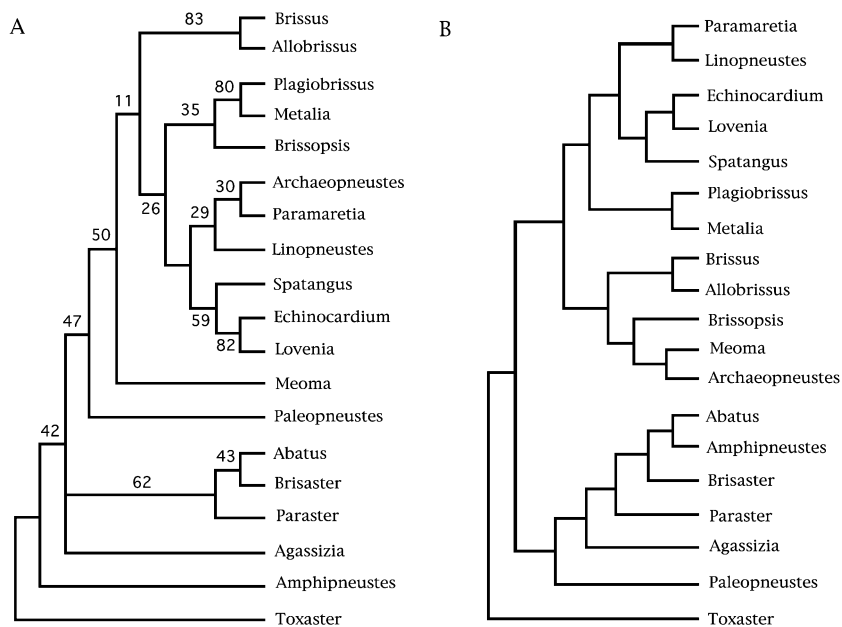


**Fig. 1** A, B. Trees derived from parsimony analysis of morphological data matrix presented in the Appendix. —A. Topology generated from analysis of a data matrix of just the 18 ingroup genera for which we had complementary molecular data. —B. Topology obtained from parsimony analysis of the full data set of 88 taxa with *a posteriori* weighting according to maximum rescaled consistency index. Taxa for which no complementary molecular data are available have been stripped out.

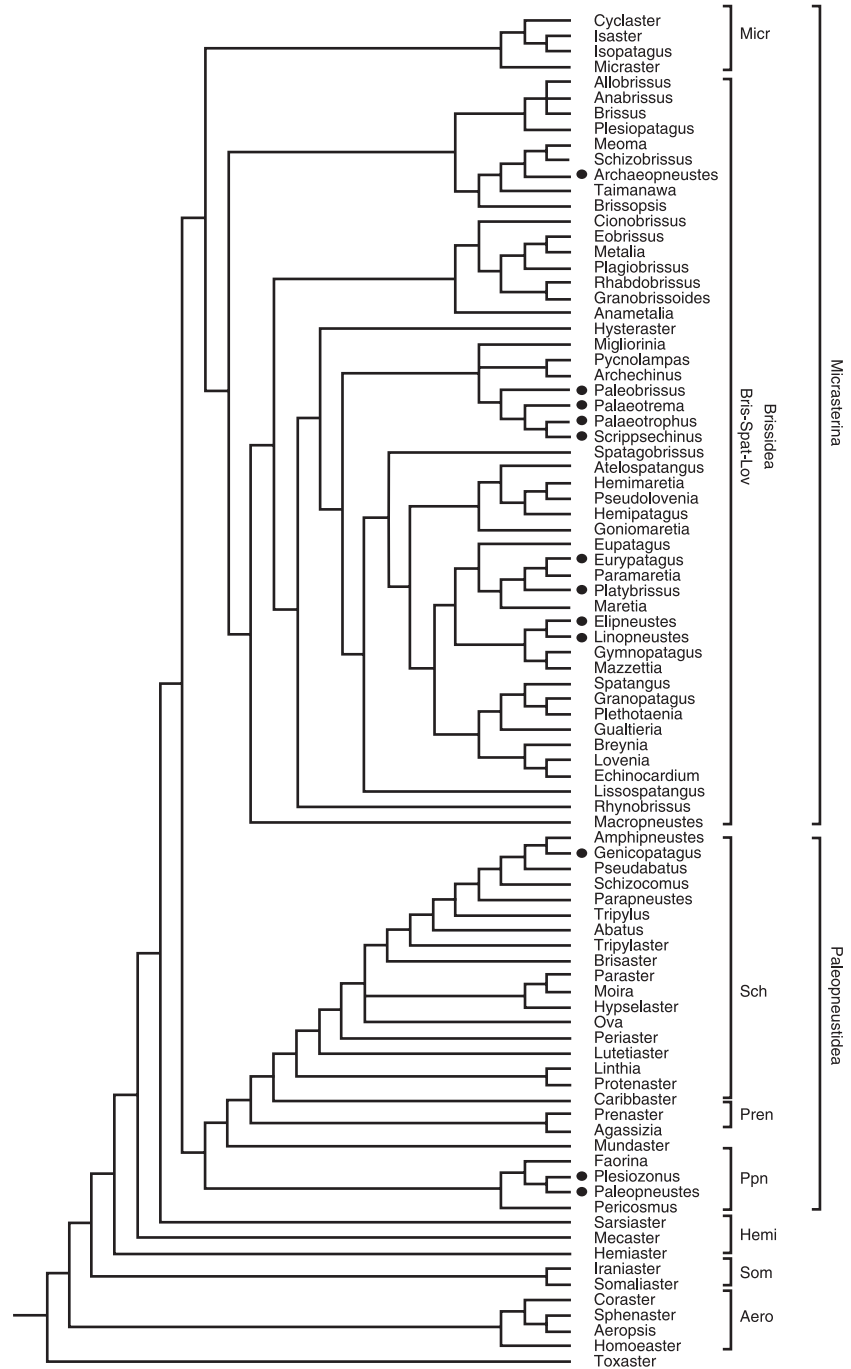


**Fig. 2** Strict consensus tree derived from morphological data matrix presented in Appendix for full data set of 89 taxa. *Abbreviations:* Aero — Aeropsidae; Bris — Brissidae; Hemi — Hemiasteridae; Lov — Loveniidae; Micr — Micrasteridae; Ppn — Paleopneustidae; Sch — Schizasteridae; Som — Somaliasteridae; Spat — Spatangidae; Tox — Toxasteridae; Pren — Prenasteridae. Filled circles indicate taxa placed in the Sub-order Asterostomatina by Fischer (1966).

**Molecular results**

Parsimony analyses on each partial gene sequence generated trees which, when compared pairwise, passed Farris *et al.*'s (1994) test of congruence. Consequently, we combined the three gene sequences into a single molecular data matrix for all subsequent analyses. Bayesian, likelihood and parsimony analyses were all applied to the combined data and generated similar but not identical results (Fig. 3).

Bayesian and ML analyses generated identical results, differing only in resolution (Fig. 3). Both fail to identify a clade corresponding to the Schizasteridae, although *Amphipneustes*, *Abatus* and *Brisaster* are grouped together. The Brissidae, Spatangidae and Loveniidae are identified as a clade with high support. Within this there are three clades: *Meoma* and *Archaeopneustes* group together with high support, as do *Brissus*, *Allobrissus* and *Brissopsis*. A third large clade consists of

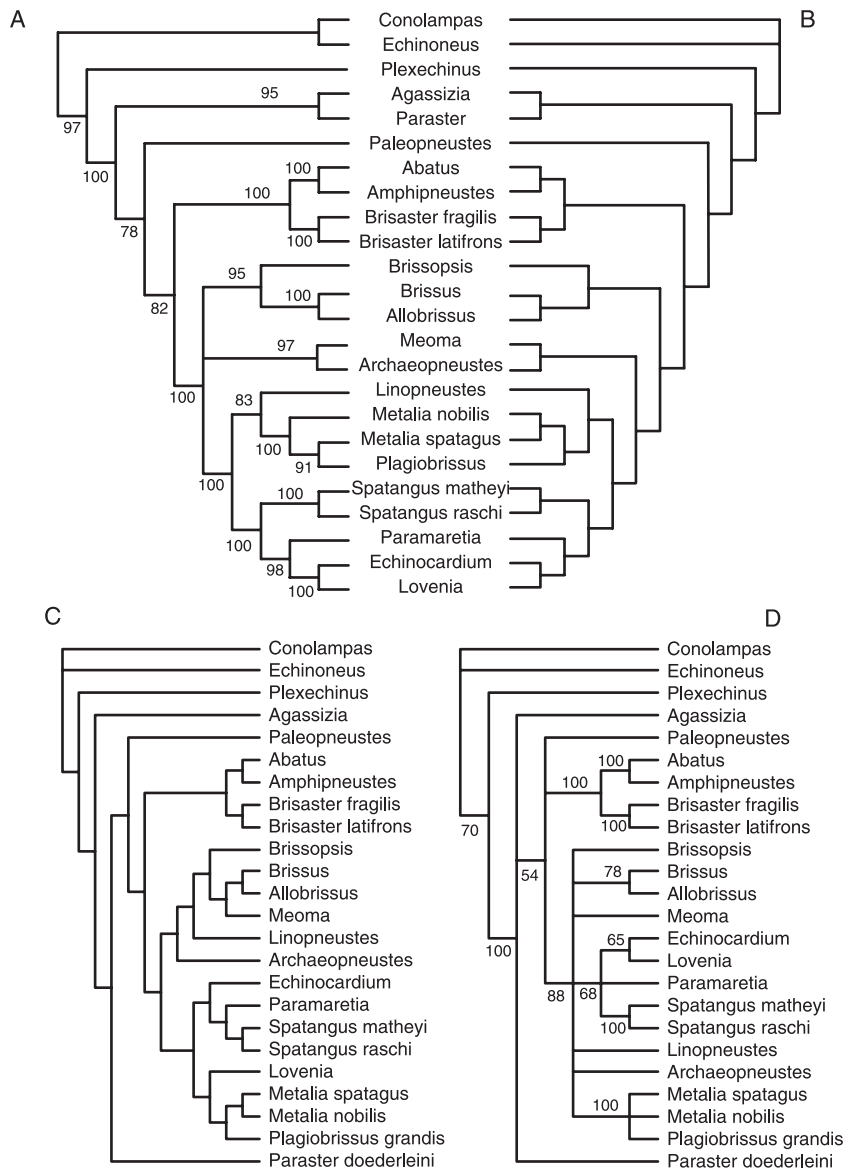


**Fig. 3** A–D. Trees derived from the combined 28S rRNA, 16S rRNA and COI gene sequences using —A. Bayesian analysis, —B. maximum likelihood and (C, D) maximum parsimony (see text for details). —C. most parsimonious tree; —D. Bootstrap tree based on 500 replicates each with 10 random additions.

*Linopneustes*, *Spatangus*, *Paramaretia*, *Lovenia*, *Echinocardium*, *Plagiobrissus*, *Metalia* and *Linopneustes*. *Metalia* and *Plagiobrissus* group together with high support, as do *Spatangus*, *Paramaretia*, *Echinocardium* and *Lovenia*. The parsimony tree (Fig. 3), however, differs markedly from ML and Bayesian trees. Templeton's test indicates that the parsimony, Bayesian and likelihood trees derived from the molecular data are not seriously in conflict and could all represent suboptimal estimates of the same underlying topology (Table 5).

**Comparison of molecular and morphological phylogenetic estimates**

For the reduced dataset, the trees derived for morphological and molecular data are incompatible with one another under

a Templeton's test (Table 5). However, when the morphological tree is constructed from the full dataset of 88 taxa and characters are reweighted according to their initial rescaled consistency index, then the comparison between morphological and molecular estimates based on ML or Bayesian analysis becomes very much closer (Fig. 4) and they pass a Templeton's test of congruence (Table 5). However, there is still disagreement as to many of the deeper relationships. Of the two data sets, molecular data is strongly incongruent with the morphological trees, but the morphological data fits both morphological and molecular trees almost equally as well. None of the nodes that are in disagreement are strongly supported by high values in bootstrap or Bremer support analyses.

**Table 5** Results of Templeton's Wilcoxon signed-ranks test assessing the congruence of alternative topologies derived from molecular and morphological analyses. *N* = Number of variable characters, *z* = correction factor, *P* = probability.

Tree	Length	Rank sums	<i>N</i>	<i>z</i>	<i>P</i>
1	1776	(best)			
2	1791	2578.0 -1887.0	94	-1.4783	0.1393
3	1787	2690.0 -2161.0	98	-1.0642	0.2872
4	1902	10590.0 -2290.0	160	-7.6097	< 0.0001*
5	1829	6256.0 -3060.0	136	-3.7741	0.0002*

**Molecular trees vs. morphological trees**

Tree 1: best tree, generated from the three gene molecular data set by maximum parsimony (MP) optimality criterion

Tree 2: best tree, generated from the three gene molecular data set by maximum likelihood (ML) optimality criterion

Tree 3: best tree, generated from the three gene molecular data set by Bayesian optimality criterion

Tree 4: generated from the morphological data set of 88 fossil and Recent taxa, with a parsimony (MP) optimality criterion

Tree 5: generated from the morphological data set of 22 Recent taxa, with a MP optimality criterion

Tree	Length	Rank sums	<i>N</i>	<i>z</i>	<i>P</i>
1	181.60	(best)			
2	188.93	129.0 -61.0	19	-1.4532	0.1462
3	190.26	137.5 -52.0	19	-1.9076	0.0564
4	190.26	137.5 -52.5	19	-1.9076	0.0564

**Tree based on all taxa vs. molecular trees**

Tree 1: best tree, generated from the morphological data set of 88 fossil and Recent taxa

Tree 2: generated from the three gene molecular data set by MP optimality criterion

Tree 3: generated from the three gene molecular data set by ML optimality criterion

Tree 4: generated from the three gene molecular data set by Bayesian optimality criterion

Tree	Length	Rank sums	<i>N</i>	<i>z</i>	<i>P</i>
1	169.61	(best)			
2	188.93	280.0 -71.0	26	-2.7485	0.0060*
3	190.26	319.0 -87.0	28	-2.7320	0.0063*
4	190.26	319.0 -87.0	28	-2.7320	0.0063*

**Tree based on 18 core genera (22 species) vs. molecular trees**

Tree 1: best tree, generated from the morphological data set of 22 Recent taxa

Tree 2: generated from the three gene molecular data set by MP optimality criterion

Tree 3: generated from the three gene molecular data set by ML optimality criterion

Tree 4: generated from the three gene molecular data set by Bayesian optimality criterion

**Discussion**

Congruence between independent data sets is the best guide to whether our phylogenetic tree is accurately reconstructed (De Queiroz *et al.* 1995). Although there are some remaining problems of mismatch between the results generated from

morphological and molecular data, it is clear that much closer correspondence is achieved between these two independent estimates of phylogenetic relationships when the morphology of a relatively comprehensive dataset of Recent and fossil taxa is analysed by parsimony, and

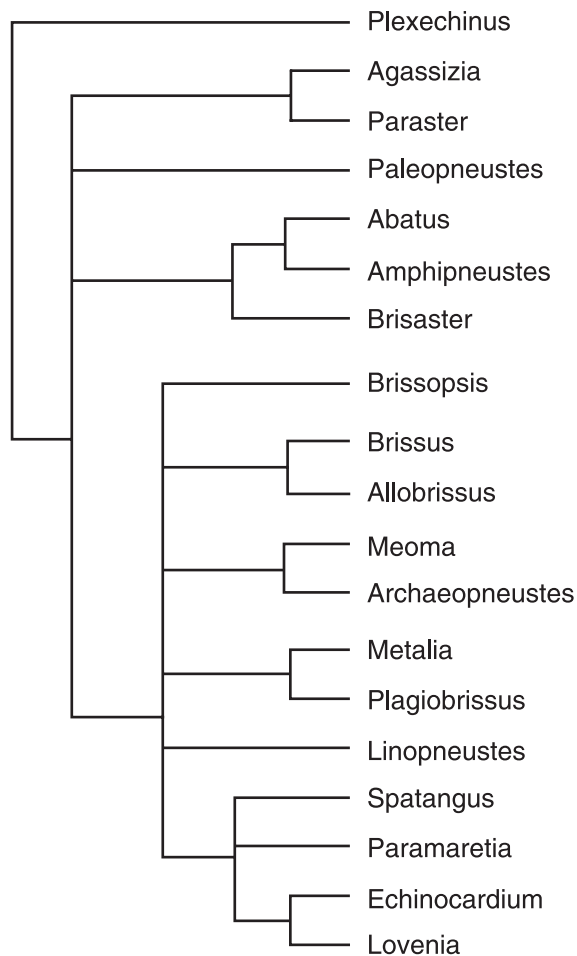


**Fig. 4** Clades well supported by morphological and molecular trees (molecular data based on all three genes combined; morphological tree based on analysis of 88 taxa). Thick lines = nodes present in both morphological and molecular analyses. Thin line = node with high support in molecular analysis and just suboptimal in morphological analysis.

homoplasy of characters is taken into account by *a posteriori* reweighting.

The results are not identical, but are sufficiently close that the two estimates pass a Templeton's test of congruence in both directions. By contrast, when our phylogenetic analysis of morphological data was restricted to just the small number of taxa for which molecular data are available, results were incongruent, and the two independent estimates of phylogenetic relationships appeared to be in conflict. Therefore, in this case, we believe that model-based analyses of molecular data and parsimony-based analyses of morphological characters densely sampled across taxa with *a posteriori* weighting provide our most accurate phylogenetic hypothesis of spatangoid relationships.

What then might be causing the differences between our molecular and morphological estimates? First, the results generated from the molecular data are to some degree sensitive to the analytical technique used and the initial assumptions made. Parsimony, likelihood and Bayes analyses incorporated successively more specific models of evolution and did not produce the same topology (Fig. 3). However, the two methods that weighed transversions as less likely than transitions generated congruent trees.

Sampling density, in the form of either taxon sampling or gene sampling, probably lies at the root of the differences we have observed between our morphological and molecular analyses. Previous studies (e.g. Hillis 1996, 1998; Givnish & Sytsma 1997) have focused on the role of character sampling and have emphasized that greater accuracy is achieved as more characters are added to an analysis. Although this certainly applies to molecular data, it is less obvious that this is also the case for morphological data (Lambooy 1994; Wiens & Hillis 1996; Scotland *et al.* 2003). Here, taxon sampling may have a more potent effect on a tree. Rosenberg & Kumar (2001) argued that for molecular datasets incomplete taxonomic sampling was unlikely to generate misleading results as long as sufficiently large numbers of variable characters were available. By contrast, morphologists have argued that denser sampling of taxa, especially fossil taxa, is of great importance for tree accuracy (Gauthier *et al.* 1988; Smith 1998; Wills *et al.* 1998; Poe 1998).

The importance of dense taxon sampling is evident from our morphological data. The results that we obtained from parsimony analysis of the reduced dataset are significantly different from both the molecular estimates and the estimate based on a much denser sampling of taxa. In this case, sparse sampling is exacerbated by another factor: many of the deep-sea groups appear to have undergone secondary morphological simplification involving the loss of fascioles and reduction or complete loss of petals.

Fascioles are essential structures for an infaunal mode of life, providing both a pump for ciliary driven water currents within the burrow and a mucous sheath for binding the burrow walls (Lawrence 1987). However, they serve no purpose in epibenthic species and are therefore commonly lost in deep-sea forms. Similarly, the highly developed respiratory zones of tube feet that form the petals are essential for shallow water spatangoids, but are commonly simplified or absent in deep-sea representatives where respiratory needs are less demanding and the body wall much thinner. With limited taxon sampling, the absence of petals and fascioles is interpreted as plesiomorphic and such taxa are pulled to a basal position. When denser sampling, that includes the immediate fasciole-bearing and petaloid sister groups to the deeper water taxa (many of which are fossil), is available, such absences are recognized as being secondary reversals and a different topology results.

A key point worth emphasizing is that adding more taxa reduces the character to taxon ratio for morphological traits but may improve the accuracy of the tree topology. Therefore, the number of taxa sampled could be of greater importance to tree accuracy than the number of characters per taxon, contrary to the assertion of Scotland *et al.* (2003).

### Comparative character homoplasy

Table 6 summarizes the levels of homoplasy and informativeness of morphological and molecular characters as optimized onto their respective topologies. The morphological characters used in this study have been divided up into suites of related structures to allow comparative analysis.

The first point of interest is that homoplasy levels are lowest overall in the reduced dataset morphological analysis and highest in the all taxon morphological data set analysis, with molecular data intermediate. Thus although the reduced dataset appears

**Table 6** Homoplasy levels for molecular characters for the three genes, individually and in combination, optimized onto the molecular trees based on parsimony and maximum likelihood (ML) optimization criteria. For morphological characters, optimized onto the topologies derived from the 18 core ingroup taxa (reduced taxon tree) and for the full 88 taxon dataset. HI = Homoplasy Index; RI = Retention Index; RC = Rescaled Consistency Index; pst/ppt = peristome and periproct.

	Number of characters	Number of informative characters	HI	RI	RC
<b>MOLECULES</b>					
<b>Parsimony tree</b>					
COI	2227	465	0.59	0.44	0.20
16S	633	209	0.61	0.37	0.15
28S	493	138	0.53	0.48	0.23
<b>ML tree</b>					
COI	2227	465	0.59	0.44	0.20
16S	633	209	0.61	0.36	0.14
28S	493	138	0.58	0.47	0.22
28S	1099	118	0.49	0.57	0.35
<b>MORPHOLOGY</b>					
<b>Reduced taxon tree</b>					
All characters	79	52	0.53	0.58	0.30
Apical disc	7	4	0.47	0.42	0.22
Ambulacra	25	18	0.57	0.51	0.22
Oral lambs	14	10	0.43	0.64	0.37
pst/ppt	7	2	0.57	0.27	0.12
Fascioles	19	13	0.38	0.76	0.47
Tubercles	7	5	0.46	0.60	0.32
<b>All taxon tree</b>					
All characters	79	69	0.80	0.66	0.14
Apical disc	7	6	0.76	0.68	0.16
Ambulacra	25	22	0.83	0.57	0.10
Oral lambs	14	13	0.79	0.74	0.16
pst/ppt	7	5	0.78	0.50	0.10
Fascioles	19	17	0.74	0.75	0.20
Tubercles	7	6	0.78	0.60	0.13

to be performing better than the molecular data in terms of character informativeness, this is achieved because of a great deal of homoplasy has been hidden by low sampling density.

Amongst molecular datasets the 28S gene, though providing slightly fewer parsimony informative characters than other genes, has the lowest levels of homoplasy and highest Rescaled Consistency and Retention Indices, while the COI gene has the reverse. For the divergences we are interested in, the 28S gene is providing the most informative data.

Morphological characters drawn from different anatomical structures of the test show very similar overall levels of homoplasy, but with fasciole distribution showing the lowest and ambulacral plating the highest. Given the small differences, there is no justification for preferring one particular anatomical set of features over any other when constructing a spatangoid phylogeny.

### Taxonomic implications and recommendations

Because morphological and molecular approaches only partially agree, even when a large number of taxa is included in the morphological character analysis, only those branches supported by both morphological and molecular data are considered robust. Figure 4 is a consensus tree that shows those branches seen in both morphological and molecular analyses (thick lines), plus one clade that is very strongly supported by molecular data (100% in the Bayesian analysis) but which is suboptimal in the morphological analysis (thin line). We have based our conclusions about spatangoid taxonomy and phylogenetic relationships on this tree. In addition, we make a few comments based solely on our analysis of the Recent and fossil morphological analysis.

**1** The grouping together of spatangoid taxa that lack fascioles as adults into Mortensen's Palaeopneustidae or Fischer's Asterostomatina has historically been regarded as unsatisfactory (Fischer 1966; Chesher 1968) and is strongly rejected by our results. Molecular data demonstrate that three members of Fischer's (1966) Asterostomatina (*Paleopneustes*, *Linopneustes* and *Archaeopneustes*) each have a different non-asterostomatid sister group (Fig. 1). Twelve genera of Asterostomatina that were included in the full morphological dataset are scattered across the cladogram, forming six unrelated clades (Fig. 2). Four of these clades lie within the Brissidea clade and two within the Paleopneustina clade. Chesher's (1968) removal of two Asterostomatina (*Paleopneustes* and *Plesiozonus*) to a paleopneustid clade that also includes *Pericosmus* and *Faorina* is supported by our morphological analysis. However, his suggestion that the remaining members form the family Asterostomatidae is contradicted.

The remaining asterostomatid taxa do, however, include one well-defined clade – the taxa *Palaeobrissus*, *Paleotrema*, *Palaeotrophus* and *Scrippsechinus* – which corresponds to Mortensen's subfamily Palaeotrematinae. The polyphyletic

arrangement of the fasciole-less ‘asterostomatid’ spatangoids highlighted by both molecular and morphological analyses strongly implies that there were multiple origins for these deep-sea spatangoids.

**2** The Toxasteridae are confirmed as a basal grade, as was also clearly demonstrated by the work of Villier *et al.* (2004). The more detailed and denser sampling of toxasterids in that paper provides the best phylogenetic hypothesis for how these primitive taxa are related. However, we found no support for their grouping of Hemiasteridae and Schizasteridae into a monophyletic Hemiasterina. By contrast, the taxa currently placed in Hemiasteridae form a paraphyletic grade in our analysis.

**3** Just two large clades make up the great majority of modern spatangoids, both of which have origins around the mid-Cretaceous. These correspond to the brissid–spatangid–loveniidi clade and the paleopneustid–prenosteriid–schizasterid clade. The former is here referred to as the Superfamily Brissidea nov., while the latter was named Paleopneustoidea by Markov & Solovjev (2001: 80).

**4** Fischer’s (1966) detailed placement of taxa within the Brissidea into the families Spatangidae, Brissidae and Loveniidae finds little support. Although there are core clades that include elements of each family, the specific taxa Fischer assigned to each lie scattered throughout the Brissidea. Morphological and molecular data strongly argue for a core Brissidae that includes *Brissus* and *Brissopsis*, and a core Loveniidae that includes *Lovenia* and *Echinocardium*. There is also a core of taxa corresponding to Mortense’s (1951) subfamily Maretiinae. *Meoma*, which has a rather different fasciole pattern to other brissids (Smith & Stockley 2005) is basal to both as well as to another clade of brissid taxa uniting *Metalia* and *Plagiobrissus*. However, it is evident from both morphological and molecular analyses that the Brissidae as constituted by Fischer (1966) represents a basal grade. A major focus for future work will be to establish with greater confidence the relationships of the various genera of Brissidea.

**5** The sister group to the Brissidea is formed by the Micrasteridae, which includes two living representatives, *Cyclaster* and *Isopatagus*. Micrasterids differ from Brissidea in two important characters: the detailed pathway taken by the subanal fasciole and the ambulacral plate bordering the rear of the sternal plate.

**6** The Paleopneustidea have traditionally been separated into two clades, the Palaeopneustidae (*Pleziozonus*, *Paleopneustes*, *Pericosmus* and *Faorina*), and the Schizasteridae. Morphology and some molecular analyses identify these as sister taxa, but other molecular analyses place *Paleopneustes* within the schizasterid taxa. Neither grouping is strongly supported. There is a more serious conflict in the relative positioning of *Paraster*. Morphological data support *Agassizia* as the most basal and group *Amphipneustes*, *Abatus*, *Brisaster* and *Paraster* together, whereas molecular data consistently place *Paraster*

as sister taxon to *Agassizia*. Denser sampling of taxa for both morphological and molecular analysis is required to resolve relationships in this part of the tree.

**7** There are two small clades with living representatives that are more basal to the Paleopneustoidea plus Micrasterina. Mortensen’s and Fischer’s Hemiasteridae is, like their family Toxasteridae, a paraphyletic grade group near the base of the spatangoid cladogram and includes the modern genus *Sarsiaster*.

Mortensen’s Aeropsidae contains two extant taxa but may be diphyletic. *Aeropsis* itself belongs to a clade that includes the late-Cretaceous–early Palaeogene corasterids such as *Sphenaster* and *Coraster*. The other genus that Mortensen included, *Aceste*, is very different in appearance and may represent a highly derived schizasterid close to *Brisaster*. The Aeropsidae are more derived than the Palaeostomatidae.

### Acknowledgements

We are indebted to the following people, who kindly provided tissue samples for molecular analysis: Owen Anderson, Mike Hart, Sonoko Kinjo, Benedicte Lafay, Chuck Messing, Rich Mooi, Matt Richmond, Patrick Schembri, Jon Todd, Paul Tyler and Craig Young. We would also like to thank the following for access to museum holdings and type material, Sheila Halsey (Natural History Museum, London), Dave Pawson and Jan Thompson (Smithsonian Institution), Fred Collier (Museum of Comparative Zoology, Harvard University), Agnes Rage (Museum National d’Histoire Naturelle, Paris), Claus Nielsen (Zoological Museum, University of Copenhagen). We also thank Rich Mooi and an anonymous referee for their helpful comments.

### References

- Bremer, K. (1994). Branch support and tree stability. *Cladistics*, *10*, 295–304.
- Chesher, R. H. (1968). The systematics of sympatric species in West Indian spatangoids: a revision of the genera *Brissopsis*, *Plethotaenia*, *Paleopneustes*, and *Saviniaster*. *Studies in Tropical Oceanography*, *7*, 1–168, pls 1–35.
- Cunningham, C. W. (1997). Can three incongruence tests predict when data should be combined? *Molecular Biology and Evolution*, *14*, 733–740.
- De Queiroz, A., Donoghue, M. J. & Kim, J. (1995). Separate versus combined analysis of phylogenetic evidence. *Annual Reviews in Ecology and Systematics*, *26*, 657–681.
- Durham, J. W. & Melville, R. V. (1957). A classification of echinoids. *Journal of Paleontology*, *31*, 242–272.
- Farris, J. S., Källersjö, M., Kluge, A. G. & Bult, C. (1994). Testing significance of incongruence. *Cladistics*, *10*, 315–319.
- Fischer, A. G. (1966). Spatangoida. In R. C. Moore (Ed.) *Treatise on Invertebrate Paleontology. Part U, Echinodermata 3* (pp. U543–628). Boulder, CO: University of Colorado and Geological Society of America.
- Gauthier, J., Kluge, A. G. & Rowe, T. (1988). Amniote phylogeny and the importance of fossils. *Cladistics*, *4*, 105–209.

- Ghiold, J. (1988). Species distributions of irregular echinoids. *Biological Oceanography*, 6, 79–162.
- Ghiold, J. & Hoffman, A. (1989). Biogeography of spatangoid echinoids. *Neue Jahrbuch für Geologie und Paläontologie Abhandlungen*, 178, 59–83.
- Givnish, T. J. & Sytsma, K. J. (1997). Consistency, characters and the likelihood of correct phylogenetic inference. *Molecular Phylogenetics and Evolution*, 7, 320–330.
- Hillis, D. M. (1996). Inferring complex phylogenies. *Nature*, 383, 140–141.
- Hillis, D. M. (1998). Taxonomic sampling, phylogenetic accuracy, and investigator bias. *Systematic Biology*, 47, 3–8.
- Huelsenbeck, J. P. & Ronquist, F. (2003). *MrBayes (Bayesian analysis of phylogeny)*, Version 3.0B4. Computer program distributed by the authors.
- Janies, D. (2001). Phylogenetic relationships of extant echinoderm classes. *Canadian Journal of Zoology*, 79, 1232–1250.
- Jeffery, C. H. (1999). A reappraisal of the phylogenetic relationships of somaliasterid echinoids. *Palaeontology*, 42, 1027–1041.
- Jeffery, C. H., Emlet, R. B. & Littlewood, D. T. J. (2003). Phylogeny and evolution of developmental mode in temnopleurid echinoids. *Molecular Phylogenetics and Evolution*, 28, 99–118.
- Kerr, A. M. & Kim, J. H. (2001). Bi-penta-bi-decaradial symmetry: a review of evolutionary and developmental trends in Holothuroidea (Echinodermata). *Journal of Experimental Zoology (Molecular, Developmental, Evolutionary)*, 285, 93–103.
- Lafay, B., Smith, A. B. & Christen, R. (1995). A combined morphological and molecular approach to the phylogeny of asteroids (Asteroidea: Echinodermata). *Systematic Biology*, 44, 190–208.
- Lamboy, W. F. (1994). The accuracy of maximum parsimony method for phylogenetic reconstruction with morphological characters. *Systematic Botany*, 19, 489–505.
- Larson, A. (1994). The comparison of morphological and molecular data in phylogenetic systematics. In B. Schierwater, B. Streit, G. P. Wagner & R. De Salle (Eds) *Molecular Ecology and Evolution: Approaches and Applications* (pp. 371–390). Basel: Birkhäuser-Verlag.
- Lawrence, J. M. (1987). *A Functional Biology of Echinoderms*. London & Sydney: Croom-Helm.
- Littlewood, D. T. J. & Smith, A. B. (1995). A combined morphological and molecular phylogeny for echinoids. *Philosophical Transactions of the Royal Society, London B*, 347, 213–234.
- Littlewood, D. T. J., Smith, A. B., Clough, K. A. & Ensom, R. H. (1997). The interrelationships of the echinoderm classes: morphological and molecular evidence. *Biological Journal of the Linnean Society*, 61, 409–438.
- Maddison, D. R. & Maddison, W. P. (2001). *Macclade 4. Analysis of Phylogeny and Character Evolution*, Version 4.03. Sunderland, MA: Sinauer Associates.
- Markov, A. V. & Solovjev, A. N. (2001). Echinoids of the family Paleopneustidae (Echinoidea, Spatangoida): morphology, taxonomy, phylogeny. *Geos*, 2001, 1–109.
- Mortensen, T. (1950). *A monograph of the Echinoidea. V. 1 Spatangoida. I*. Copenhagen: C. A. Reitzel.
- Mortensen, T. (1951). *A monograph of the Echinoidea. V. 1 Spatangoida. II*. Copenhagen: C. A. Reitzel.
- Neraudeau, D., David, B. & Madon, C. (1998). Tuberculation in spatangoid fascioles: delineating plausible homologies. *Lethaia*, 31, 323–334.
- Poe, S. D. (1998). Sensitivity of phylogenetic estimation to taxonomic sampling. *Systematic Biology*, 47, 18–31.
- Posada, D. & Crandall, K. A. (1998). MODELTEST: testing the model of DNA substitution. *Bioinformatics*, 14, 817–818.
- Rosenberg, M. S. & Kumar, S. (2001). Incomplete taxon sampling is not a problem for phylogenetic inference. *Proceedings of the National Academy of Sciences USA*, 98, 10751–10756.
- Scotland, R. W., Olmstead, R. G. & Bennett, J. R. (2003). Phylogeny reconstruction: The role of morphology. *Systematic Biology*, 52, 539–548.
- Smith, A. B. (1998). What does palaeontology contribute to systematics in a molecular world? *Molecular Phylogenetics and Evolution*, 9, 437–447.
- Smith, A. B. (2004). *The Echinoid Directory*. [electronic publication] <http://www.nhm.ac.uk/palaeontology/echinoids>.
- Smith, A. B., Littlewood, D. T. J. & Wray, G. A. (1995a). Comparing patterns of evolution: larval and adult life-history stages and small ribosomal RNA of post-Palaeozoic echinoids. *Philosophical Transactions of the Royal Society, London B*, 349, 11–18.
- Smith, A. B., Patterson, G. L. & Lafay, B. (1995b). Ophiuroid phylogeny and higher taxonomy: morphological, molecular and palaeontological perspectives. *Zoological Journal of the Linnean Society*, 114, 213–243.
- Smith, A. B., Peterson, K. J., Wray, G. & Littlewood, D. T. J. (2004). From bilateral symmetry to pentaradiality: The phylogeny of hemichordates and echinoderms. In J. Cracraft & M. Donoghue (Eds) *The Tree of Life* (pp. 365–383). Oxford: Oxford University Press.
- Smith, A. B. & Stockley, B. (2005). Fasciole pathways in spatangoid echinoids: a new source of phylogenetically informative characters. *Zoological Journal of the Linnean Society*, 143, in press.
- Smith, A. B. & Wright, C. W. (1999). British Cretaceous echinoids. Part 5, Holecypoida, Echinoneoidea. *Monograph of the Palaeontographical Society, London* pp. 343–390, pls 115–129 (publication number 612, part of vol. 153).
- Swofford, D. L. (2002). *PAUP\*. Phylogenetic Analysis Using Parsimony (and Other Methods)*, Version 4. Sunderland, MA: Sinauer Associates.
- Villier, L., Neraudeau, D., Clavel, B., Neumann, C. & David, B. (2004). Phylogeny of early Cretaceous spatangoids (Echinodermata: Echinoidea) and taxonomic implications. *Palaeontology*, 47, 265–292.
- Wiens, J. J. & Hillis, D. M. (1996). Accuracy of parsimony analysis using morphological data: a reappraisal. *Systematic Botany*, 21, 237–243.
- Wills, M. A., Briggs, D. E. G., Fortey, R. A., Wilkinson, M. & Sneath, P. H. A. (1998). An arthropod phylogeny based on fossil and Recent taxa. In G. D. Edgecombe (Ed.) *Arthropod Fossils and Phylogeny* (pp. 33–106). New York: Columbia University Press.

## Appendix 1 Morphological characters and character state definitions used in this paper

### 1–7. Apical disc

The apical disc in spatangoids comprises five ocular plates and from one to four genital plates (Fig. 5). These form and take on their definitive arrangement early in ontogeny and so provide a suit of useful phylogenetic characters, as has long been recognized.

**1 Apical disc:** posterior of centre (0); subcentral to slightly anterior (1); significantly anterior of centre (2). The apical disc ranges in

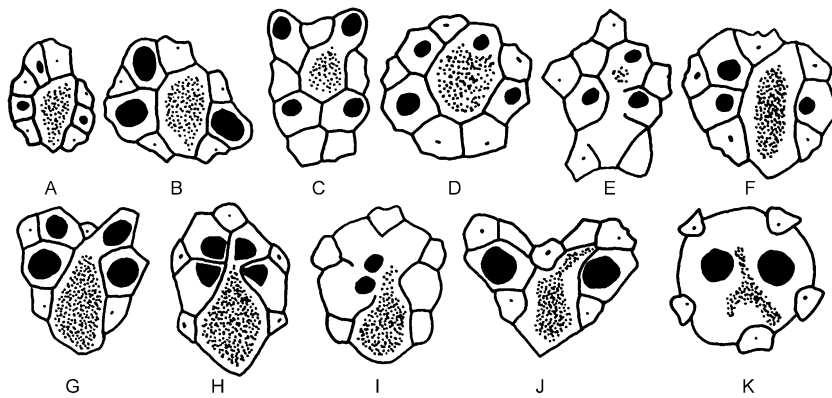


Fig. 5 A–K. Camera lucida drawings of apical disc plating in spatangoids. —A. *Abatus* (♂); —B. *Abatus* (♀); —C. *Toxaaster*; —D. *Macraster*; —E. *Paleopneustes*; —F. *Plesiozonus*; —G. *Protanaster*; —H. *Plagiobrissus*; —I. *Plesioptagus*; —J. *Ova*; —K. *Aceste*.

position from strongly anterior to posterior of mid length, along the anterior-posterior length of the test. In the majority of spatangoids, the anterior ocular plate is slightly anterior of mid length. The position of the apical disc has been measured in plan view as the distance from the anterior border to ocular plate III. If this is 35% or less than the total test length in adults it is scored as significantly anterior of centre, while if it is 60% or more it is scored as posterior.

**2 Number of genital pores:** four (0); three (no opening in genital plate 2) (1); three (no opening in genital plate 3) (2); two (no gonopores in the anterior genital plates) (3); two (no gonopores on the right-hand side) (4) (Fig. 5). Gonopores open through the genital plates and the number developed is independent of the number of genital plates that are present. Taxa based on individuals too young to have open gonopores are scored as unknown for this character.

**3 Apical disc plating:** *ethmophract* (0); *ethmolytic* (1). The condition in primitive spatangoids and early irregular echinoids is for all four genital plates to be in contact centrally, an arrangement termed *ethmophract* (Fig. 5C,D). However, in most spatangoids genital plate 2 is larger than other genital plates and projects posteriorly separating both the posterior oculars and the posterior genital plates. This condition is then described as *ethmolytic* (Fig. 5G).

Where the apical disc is monobasal (Fig. 5K) this has resulted from expansion of genital plate 2 and loss of the other genital plates. Clearly as the posterior ocular plates are separated, monobasal discs are scored as *ethmolytic*.

**4 Gonopores clustered close to centre rather than in outer part of genital plates:** no (0); yes (1). The relative position of gonopores on their respective genital plates varies amongst spatangoids. In most primitive spatangoids the gonopores open towards the outer (distal) point of each genital plate (e.g. Fig. 5C) or are central on small plates (Fig. 5D). However, in some the gonopores open much more centrally, on the inner part of the genital plates and so appear clustered. In this situation the anterior gonopores are separated by only a narrow calcite bridge and the hydropore zone expands to the posterior

(Fig. 7H,J). The outer part of the genital plates is then more extensive than the inner part.

**5 Size of genital pores markedly different in one individual:** no (0); yes (1). In a few taxa the anterior pair of gonopores is greatly reduced compared to the posterior pair.

**6 Sexual dimorphism (e.g. brood chambers, bivariate gonopore size distribution):** no evidence of sexual dimorphism (0); evident in gonopore size (1); evident in gonopore size and development of brooding chambers (2) [ordered]. Sexual dimorphism in spatangoids is developed only where there is lecithotrophic development and the female produces a small number of large, yolk-rich eggs that are subsequently brooded on the test. In such cases there is a clear differentiation between the small gonopores of the male and the much larger gonopore openings of the female (Fig. 5A,B). There may also be marked differences in the sunkenness of the petals; deeply sunken in females for brooding the developing embryos, and more or less flush in males. In the majority of spatangoids eggs are small, the fertilized egg develops as a dispersed planktotrophic larva, and there is no sexual dimorphism.

**7 Monobasal apical disc:** no (0); yes (1). The occurrence of a single large genital plate instead of the usual four is probably the result of expansion of genital plate 2 and resorption of genital plates 1, 3 and 4 rather than fusion.

### 8–32. Ambulacral features

**8–10. The depth of the frontal ambulacrum** There is considerable variation in how wide and how deeply indented the frontal ambulacrum is in spatangoids. Furthermore, the degree to which the frontal ambulacrum is sunken usually varies between the apex and the peristome. In some spatangoids, such as *Brisus* (Fig. 6) the anterior ambulacrum is narrow and remains flush with adjacent interambulacral zones throughout its length. In others, such as *Brisaster* (Fig. 6) the ambulacrum is wide and deeply sunken from apex to peristome. It is possible to have ambulacrum III more strongly depressed adapically than at the ambitus. In *Hemiaster*, for example, the anterior ambulacrum is weakly but distinctly depressed adapically but

this groove shallows and disappears by the ambitus. In *Moira* the frontal groove is very deep adapically and shallows markedly as it approaches the ambitus. By contrast, in *Pericosmus* the frontal ambulacrum is almost flush adapically and gradually increases in depth to the ambitus.

To encompass all this variation we use three characters, each given an initial weighting of 0.333 so that the structure of the frontal ambulacrum overall is equivalent to a single character in the analysis:

**8** *Ambulacrum III midway between apex and ambitus: flush (0); shallowly concave (1); at least as deep as wide (2).*

**9** *Ambulacrum III at ambitus: flush so that ambitus appears flat or convex in plan view (0); shallowly concave in plan view (1); at least as deep as wide forming a prominent notch in plan view (2).*

**10** *Ambulacrum III on oral surface: flush (0); shallowly concave with diffuse edges (1); forming a distinct channel with sharply defined edges (2).*

**11** *Pore-pairs: small and undifferentiated adapically, their tube-feet simple and without suckers (0); differentiated adapically and associated with enlarged funnel-building tube feet (1); laterally elongate and subpetaloid, with specialized respiratory tube-feet (2).* Adapical tube feet may be simple cylindrical structures or end in an enlarged disc. The latter are used by burrowing irregular urchins to create and maintain a connection to the surface through the sediment and may also be involved in selecting food particles. In fossil taxa the size and morphology of the associated pore-pairs in the frontal groove are used as a guide to whether adapical tube feet were specialized or not.

Only a few spatangoids have pore-pairs and tube feet of the frontal ambulacrum identical to those in the paired ambulacra on the aboral surface. Occasionally, as in *Isopneustes*, all five ambulacra are effectively petaloid and the pore-pairs in the frontal ambulacrum are laterally elongate and identical in form to those in the paired ambulacra.

**12** *Adapical tube feet of ambulacrum III: end in a blunt, rounded tip (0); penicillate (1); with wide flat-topped disc supported by a rosette of plates (2).* In most spatangoids aboral tube feet of ambulacrum III lack skeletal elements in their tip. However, in a few taxa adapical tube feet are penicillate, ending in a mass of finger-like extensions and are identical in form to the penicillate tube feet of the peristomial region. Each finger-like extension is supported by a thin calcite rod. Other spatangoids have enlarged tube feet that end in an enlarged disc supported by a rosette-like ring of calcite platelets. Fossil taxa that have small undifferentiated pore-pairs are assumed to have simple tube feet.

**13** *Frontal ambulacrum adapically: narrow, with pore-pairs close together (ambulacral plates approximately as tall as wide) (0); moderately broadened with a distinct perradial zone (ambulacral plates 1.5–5× wider than tall — e.g. *Brissopsis*, Fig. 6) (1); very wide with ambulacral plates more than 5× wider than tall (2).* This feature was measured on the aboral surface midway between the apex and ambitus.

**14** *Pores: uniserial and uniform in frontal ambulacrum (0); biserially offset in adapical region (1); pore-pairs heterogeneous (2).* Pores and tube feet in the frontal ambulacrum are generally arranged in a single column adapically. However, in some taxa tube feet can be crowded into the adapical region of the frontal ambulacra. In these forms the pores and tube feet become offset and biserially arranged. A few toxasterids have two forms of pore-pair in their anterior ambulacrum, alternately narrow and elongate. This condition is scored as a third state.

**15** *Lateral ambulacra (II and IV) on oral surface, widening close to peristome then narrowing markedly before broadening at ambitus (pinched appearance): no (0); yes (1).* The lateral ambulacral zones (II and IV) generally remain more or less parallel-sided as they approach the peristome or are only very slightly enlarged (e.g. *Archaeopneustes*, Fig. 6). But in some maretiiids and loveniids (e.g. *Lovenia*, Fig. 6) these ambulacra become strongly pinched immediately distal to the phyllode zone. The ambulacra are scored as pinched if they reduce to less than half their width immediately before the phyllodes.

**16** *Petal development: well developed with pores in each pair large and obvious and forming a pore-pair that is clearly laterally elongate and supporting leaf-like tube-feet (0); small narrow pore-pairs supporting more or less cylindrical tube-feet (1); apetaloid — pores single and tube-feet microscopic (2).*

**17** *Petals: basically cruciform (0); anterior petals widely diverging so as to be c. 180° (1); anterior petals flexed forwards so as to become subparallel to anterior ambulacrum (2).* In regular echinoids the ambulacra radiate regularly with an angle of 72° between adjacent pairs. In spatangoids, the angle between the ambulacra is more variable. Mostly anterior and posterior petals define an X-shaped pattern (e.g. *Meoma*, Fig. 6), but other patterns can be found. The anterior petals may diverge so widely that they define a nearly straight line (e.g. *Brissus*, Fig. 6), or they may be strongly flexed towards the anterior and become subparallel. Petals are classed as state 1 if the angle between the anterior petals (measured from the tips to the apical disc) is more than 160° and as state 2 if the angle is less than 50°.

**18** *Anterior petals unequal in length: no (0); yes (1).* The petals of *Nacospatangus* are unusual in having one anterior petal (ambulacrum IV) substantially longer than the other. This is clearly a derived condition.

**19** *In the anterior petals, the anterior column with about half the number of plates found in the posterior column: no (0); yes (1).* Almost all spatangoids have a strict alternating one-to-one correspondence between the plates in the two columns forming the ambulacra. The only exception to this pattern is seen in the fossil taxa *Heteraster* (1) and *Washtaster*, where the anterior column of the anterior petals is composed of approximately half the number of plates seen in the posterior column.

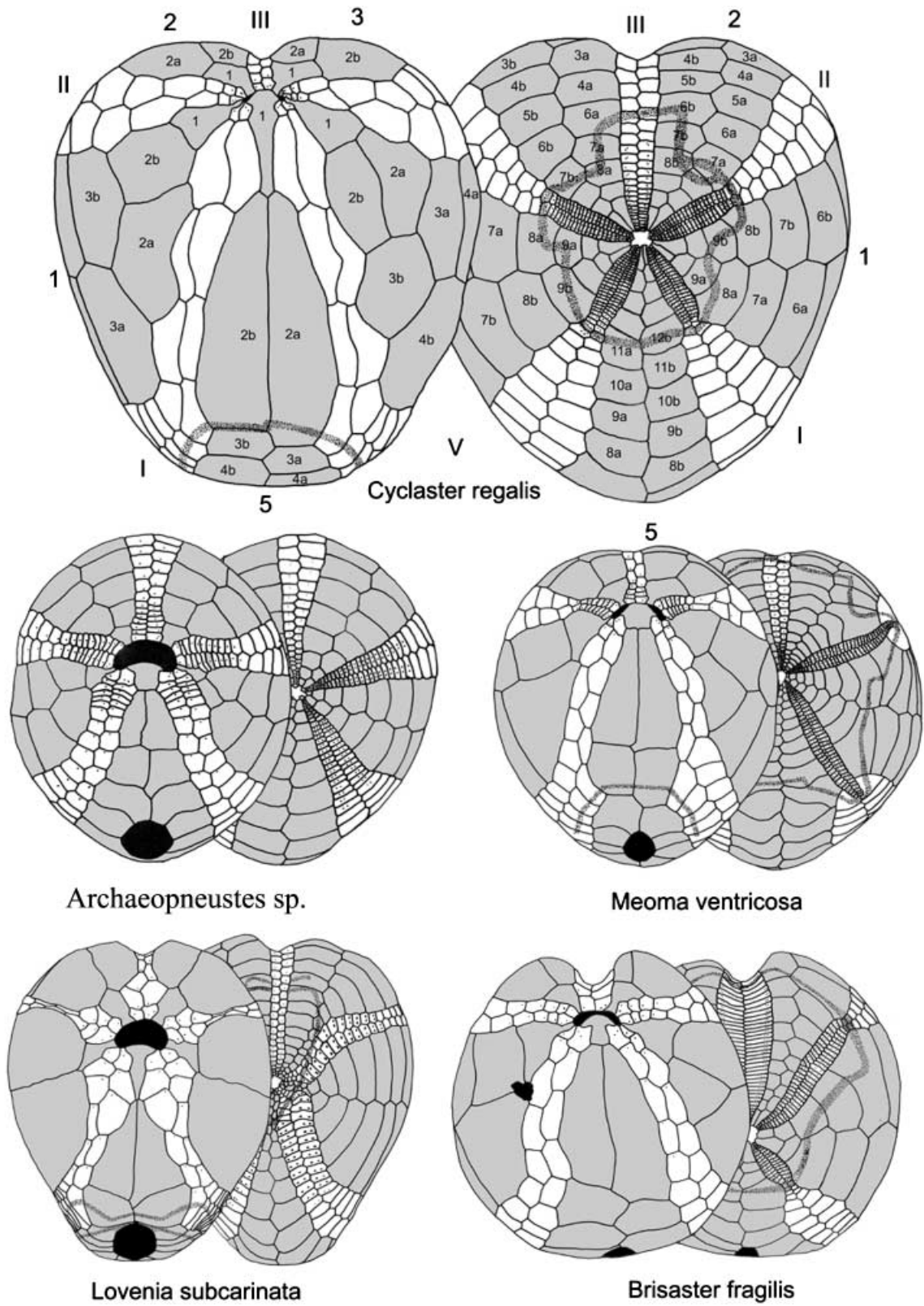
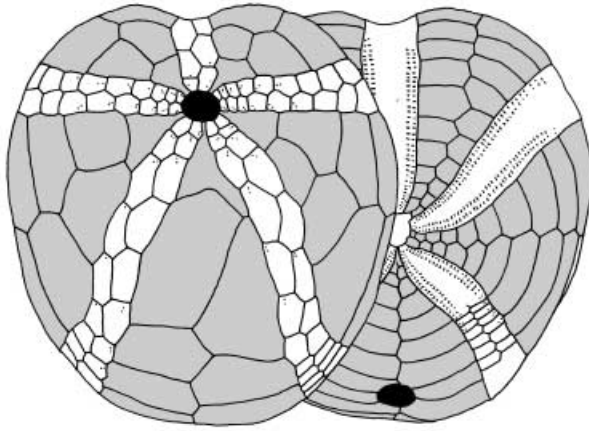
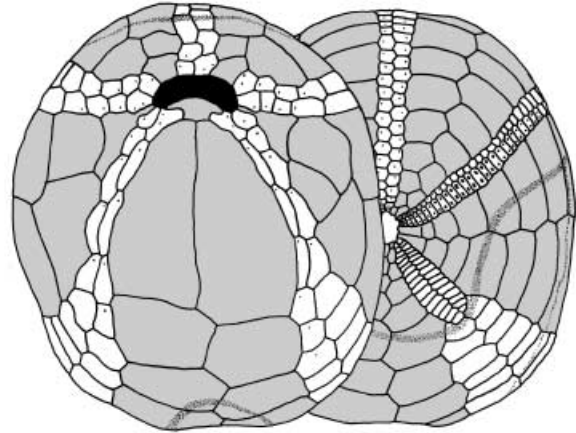


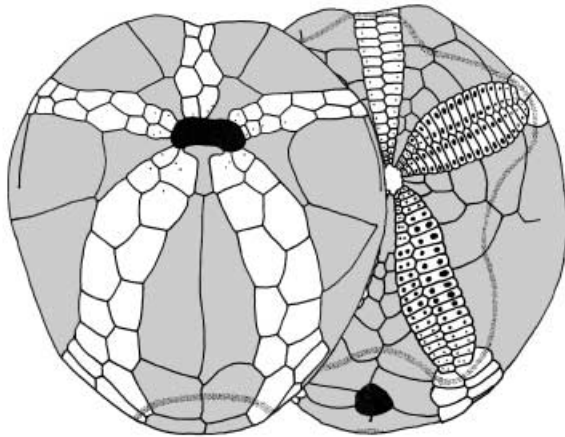
Fig. 6 Camera lucida drawings of oral (left) and aboral (right) plating in spatangoids to illustrate key morphological features scored.



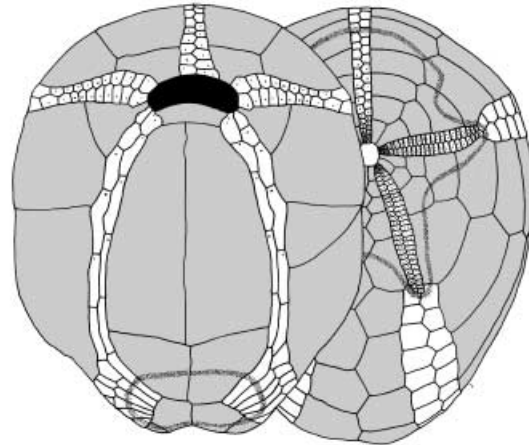
*Toxaster complanatus*



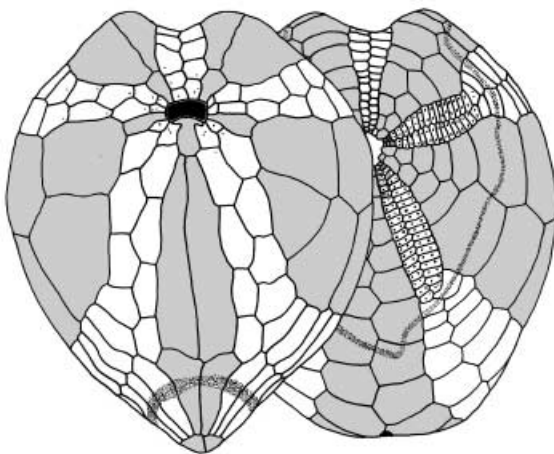
*Agassizia scrobiculata*



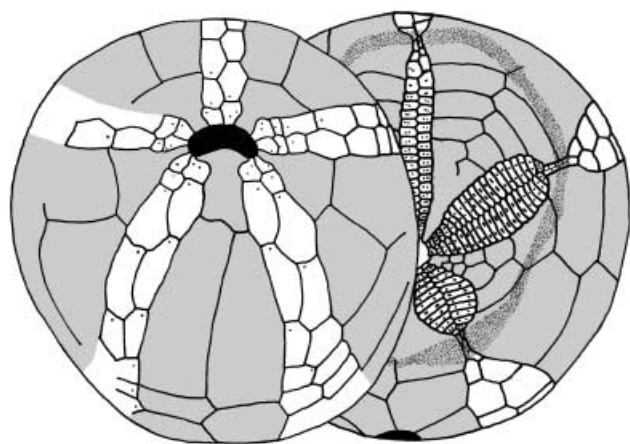
*Brissopsis pacifica*



*Brissus unicolor*



*Cinobrysis revinctus*



*Holanthus expergitus*

Fig. 6 *Continued*

**20** *Anterior and posterior petal relative lengths: subequal (0); posterior petals between 0.5 and 0.7× length of anterior petals (1); posterior petals much shorter (less than half) length of anterior petals (2); anterior petals distinctly shorter than posterior petals (< 0.8 length) (3).* There is great variability in the relative lengths of the posterior and anterior petals. Frequently, the posterior petals are shorter than the anterior petals (e.g. *Agassizia*, Fig. 6), sometimes substantially so (e.g. *Brisaster*, Fig. 6). It is also possible for the anterior petals to be distinctly shorter than the posterior petals (e.g. *Cionobrissus*, Fig. 6), or for the petals to be subequal (e.g. *Meoma*, Fig. 6).

**21** *Petals: flush (0); weakly depressed (1); deeply sunken and invaginated (2).* Petals can be flush on the surface of the test, or sunken to a greater or lesser extent, forming furrows on its surface. In some Schizasteridae the petals can be even more deeply sunken, forming a semi-enclosed cavity. Petals are scored as deeply sunken if their depth exceeds their width; they are found in the females of some sexually dimorphic species (e.g. *Amphipneustes*) [char. 6]. In such sexually dimorphic forms the depth of petals is scored only for males so as to exclude brood chambers.

**22** *Pores of Ib and IIa forming an arc laterally: no (0); yes (1).* In many Loveniidae the petals are kinked adapically such that the lateral aboral interambulacral plates reduce substantially in size near the apical disc. This results in the pores in *Ib* and *IIa* forming an almost unbroken arc (e.g. *Lovenia*, Fig. 6). Although widely present in certain genera, this character is not developed within all species and is very much dependent upon petal development. Scoring was based on the condition shown in the adult type species.

**23** *Anterior column of pore-pairs in frontal petals: rudimentary throughout (0); developed only in distal half (1); developed throughout almost their entire length, becoming rudimentary only as they approach the apex (2).* Most spatangoids do not show substantial reduction of the pore-pairs in the anterior column of the frontal petals (petals II and IV), or have only a minor asymmetry of development between anterior and posterior columns. However, pore-pairs in this column can be rudimentary in their adapical portion (e.g. *Lovenia*, Fig. 6) or throughout (e.g. *Agassizia*, Fig. 6).

**24** *Petals end in occluded plates: no (0); yes (1).* In many paleopneustids and brissids the terminal plates of the petals are reduced and occluded from the adradial suture. The terminal plates of the petals are thus enclosed by the first ambulacral plates beyond the ends of the petals (e.g. *Meoma*, Fig. 6). More usually, all ambulacral plates meet the adradial suture and there are no such occluded plates at the tips of petals (e.g. *Cyclaster*, Fig. 6).

**25** *Ambulacral zone beneath the petal ends extremely pinched: no (0); yes (1).* It is common for many spatangoids to show a slight reduction in the width of the ambulacral zones at the ends of the petals. However, in a few taxa (e.g. *Holanthus*,

Fig. 6) the reduction that occurs is very marked, and these plates are considerably less than a quarter of the width of plates in the petals or plates further towards the ambitus.

**26** *Distal termination of petals: the petal pore-pairs end abruptly (0); the petal pore-pairs decrease in size gradually and there is no abrupt end to the petals (1).*

**27** *Petal shape: the two columns parallel along their length (e.g. *Meoma*, Fig. 6) (0); petals lanceolate widened in the middle and converging distally (e.g. *Spatangus*) (1); petals gradually widening distally (e.g. *Archaeopneustes*, Fig. 6) (2).* We distinguish three basic shapes of petals amongst spatangoids, as illustrated, according to whether the pore columns remain parallel, diverge or converge towards their tip.

**28** *Anterior petal length: short, extending only about half the distance to the ambitus (0); extending between 0.6 and 0.9 of the radial length (1); reaching the ambitus in plan view (2).* The radial extent of petals is quite variable, with some taxa having petaloid zones extending more or less to the ambitus while others have short petals that extend less than half the radial distance to the ambitus. Although there seems to be more or less continuous graduation, it seems worth distinguishing forms with particularly short petals and those where the petals extend more or less to the ambitus.

**29** *Phyllode development in lateral paired ambulacra: phyllode pores/tube feet no more than 1 or 2 in a column (0); 4–7 in each column (1); 8–12 in each column (2); 13+ in each column (3).*

**30** *Pore-pairs in petals: the two columns closely spaced leaving almost no perradial zone (0); separated by more than 1.5× the pore-pair width (1).*

**31** *Ambulacral plating becomes uniserial adapically: no (0); yes (1).* In a few specialized deep-sea spatangoids the ambulacral plating becomes uniserial adapically, which is clearly a derived condition.

**32** *Subanal tube feet enlarged and with disc: no (0); yes (1).* The presence of enlarged subanal pore-pairs is used as evidence for specialized tube feet in fossil taxa.

### 33–46. Interambulacral plating and plastron characters

**33** *Number of ambulacral plate abutting rear suture of labral plate in ambulacrum I: 1 (0); 2 (1); 3 (2); 4+ (3).* The suture between the labral plate and sternal plate 5.b.2 abuts against ambulacral plates of column Ia. Here we score the ambulacral plate, numbered from the peristome (see Fig. 6) that is most commonly present in this position in adults. However, there can be a small amount of variation in this character within populations, particularly where the number is large. For example *Genicopatagus* can have ambulacral plate 4 or 5 abutting the rear of the labral plate.

**34** *Number of ambulacral plate abutting rear suture of sternal plate in ambulacrum I: 5 (0); 6 (1); 7 or 8 (2); 9+ (3); 3 or 4 (4).* This character, like char. 33, simply scores for the ambulacral plate, numbered from the peristome, that abuts the rear

suture of sternal plate 5.b.2. In Micrasterina this is very consistent, and is always ambulacral plate 6. This is independent of char. 33. Note that in Paleopneustina it can be variable within species.

**35 Suture between labral and sternal plates: straight (0); strongly curved (1).** Whereas the suture between the labral plate and sternal plates in primitive spatangoids is strongly curved (convex towards the peristome), in derived spatangoids it is more or less straight.

**36 Sternal plates, symmetrical with vertical median suture: no (0); yes (1).** The two sternal plates are distinctly asymmetrical in primitive spatangoids (e.g. *Toxaster*, Fig. 6), with plate 2b wider anteriorly and plate 2a wider at the posterior. This is the result of the median suture being strongly oblique. In derived spatangoids the suture separating the two sternal plates is more or less vertical and the two plates mirror images of each other.

**37 Labral plate: in contact with both sternal plates (0); in contact with only sternal plate 2b (1).** There are relatively few spatangids, all within the family Somaliasteridae, where the labral plate is in contact with just a single sternal plate. This is presumably a derived condition.

**38 Labral plate, disjunct: no (0); yes (1).**

**39 Episternals: biserially offset (0); paired and opposite (1).** Schizasteridae, Toxasteridae and Hemiasteridae have biserially offset episternal plates (e.g. *Cyclaster*, Fig. 6, plates 3a, 3b). By contrast, in brissids and their close relatives, the episternal plates are paired and opposite, and are mirror images of each other (e.g. *Brissus*, Fig. 6). The plates are scored as paired if the displacement between them behind the sternal plates is less than 10% of the total anterior–posterior length of the episternal plates.

**40 Sternal–episternal suture: approximately horizontal or V-d towards posterior (0); significantly convex towards the peristome (1).** Most spatangoids have approximately horizontal sternal–episternal sutures, whether the episternal plates are paired or offset. However, in taxa where the episternal plates are paired, this suture can be rather strongly flexed towards the peristome, as in *Metalia* and *Plagiobrissus*.

**41 Post-episternals: biserially offset (0); paired and weakly staggered (1); opposite (2).** The staggering (or otherwise) of the suture between the episternal plate (5.a/b.3) and the plate to the rear (plate 5.a/b.4) often follows that of the episternal/sternal plates, but not always.

**42 Ambulacral plate series in columns Vb and Ia: undifferentiated in subanal region (0); with marked change in shape of ambulacral plates such that they become transverse and geniculate behind the episternal plates (1).** In hemiasterids and toxasterids the posterior ambulacra do not vary in their overall shape or indent interambulacrum 5 on the oral surface (e.g. *Toxaster*, Fig. 6). However, in the Brissidae and Spatangidae, ambulacral plates change from being longitudinal to being laterally

enlarged, and ambulacral plate 6 in columns Ia and Vb indents the posterior interambulacrum to the rear of the episternal plates (e.g. *Cionobrissus*, Fig. 6). This is associated with the development of a subanal fasciole and subanal tube feet, but still occurs where the subanal fasciole has been secondarily lost.

**43 Lateral paired interambulacra: both amphiplacous (0); one meridoplacous, one amphiplacous (1); both meridoplacous (2).** In amphiplacous taxa the first adoral interambulacra plate abuts against two plates (e.g. *Holanthus*, Fig. 6), whereas in meridoplacous taxa it abuts distally against a single plate (e.g. *Cionobrissus*, Fig. 6). In some taxa both left and right interambulacra are meridoplacous, whereas in others the development is asymmetrical, with interambulacrum 1 amphiplacous and interambulacrum 5 meridoplacous (e.g. *Cyclaster*, Fig. 6).

**44 Plastron: widening to the rear (0); more or less parallel-sided, not narrowing markedly to rear of episternal plates (e.g. *Brissopsis*, Fig. 6) (1); strongly tapered to rear of episternal plates which make only a narrow contact with interambulacral plates to the posterior (e.g. *Cionobrissus*, Fig. 6) (2).**

**45 Lateral interambulacra on oral surface: comprise at least four or five plates (0); composed of just the basicoronal plate and the two succeeding plates (plates 2a, 2b) (1); as 1 but these plates flat so that the oral surface is planar (2).**

**46 Length of labrum: much smaller than sternal plates (0); 20–50% length of sternal plates (1); more than 50% of sternal plates in length (2).** [ordered]

#### 47–53. Peristome and periproct

**47 Peristome position: closer to the anterior border than the centre (0); subcentral (1).** Although almost all spatangoids have the peristome opening some 10–20% test length from the anterior there are a few taxa that have a more subcentral peristome. A subcentral peristome is also the condition seen in most primitive irregular echinoids although not in the immediate outgroup. The peristome is scored as subcentral if its anterior border is closer to the midlength of the test than the anterior border.

**48 Peristome shape: circular to ovate (0); distinctly pentagonal and angular (1).**

**49 Peristome orientation: downward-facing; circular or pentagonal without labral plate projecting below the plane of the opening (0); obliquely facing forwards (labral plate strongly projecting so that peristome appears C-shaped) (1); peristome vertical and almost entirely hidden in plan view by the labral plate (2).** The orientation of the peristome and the degree to which the labral plate covers the opening in oral view is a continuous variable that is here divided into three states. In many Early Cretaceous forms the peristome is a simple circular to pentagonal opening that faces directly downwards and the posterior boundary is straight or convex to the rear. However, in the majority of living forms the labral plate projects to a

variable extent over the peristomial opening. In most cases the posterior boundary of the peristome is weakly concave and the opening appears reniform. If the labral projects strongly then the anterior–posterior distance medially becomes less than half of the total length, and the opening appears C-shaped. In extreme cases the peristome can open facing forwards and is completely hidden in oral view by the labral plate.

**50** *Peristome surrounded by a distinct rim: no (0); yes (1).* The peristome in certain hemiasterids is rimmed by a very obvious lip. In most spatangoids however, the lateral and anterior margins of the peristomial border are flush and smooth.

**51** *Number of plates forming each side of the periproctal opening: two (0); three (1); four (2); five or more (3).*

**52** *Periproct tear-drop-shaped adapically: no (0); yes (1).* Most spatangoids have a circular or oval periproct. However, both *Metalia* and *Plagiobrissus* possess a periproct that narrows and elongates adapically to form a tear-drop shape.

**53** *Periproct invaginated with a distinct well leading to the sunken opening: no (0); yes (1).*

#### 54–72. Fascioles

In taxa where fascioles become obliterated and lost during ontogeny, the initial (juvenile) pattern of fasciole distribution is scored for here.

**54** *Fasciole crossing plates 4 or 5 of the posterior interambulacrum and passing orally to form a subanal ring: no (0); yes (1).*

**55** *Fasciole crossing plate 4 in posterior interambulacrum but continuing laterally as a marginal band: no (0); yes (1).* This fasciole development is usually referred to as the marginal fasciole or lateroanal fasciole.

**56** *Fasciole band crosses posterior interambulacrum along suture at rear of plates 2a/b: no (0); yes (1).*

**57** *Fasciole band crosses posterior interambulacrum midway through plates 3a/b: no (0); yes (1).*

**58** *Subanal fasciole: ovate, not enclosing strongly differentiated areas of tubercles or spines (0); bilobed, enclosing double tuft of spines (1); shield-shaped, enclosing single tuft of spines (2).* The shape of the subanal fasciole ranges from almost circular to markedly kidney-shaped; it may enclose a single or a double tuft of enlarged spines. The arrangement of tubercles within the subanal fasciole gives an unambiguous guide to spine arrangement, since there are either one or two foci of enlarged tubercles corresponding to the single or double spine tuft. The bilobed fasciole and the shield-shaped fasciole both have a clear gradient of tubercles enlarging towards either a single or a double centre. The ovate fasciole, found in Micrasteridae, has no such gradient and tubercles within the subanal fasciole are subequal in size.

**59** *Anal fasciole present: no (0); yes (1).*

**60** *Anal fasciole: independent of subanal fasciole (0); coalesced with subanal fasciole (1).* Scored as ? in forms lacking an anal fasciole.

**61** *Fasciole band (peripetalous or semipetalous) crossing between the periproct and the apical disc: absent (0); present (1).*

**62** *In interambulacrum 5 fasciole (peripetalous or semipetalous) crosses plates: 8 or 9 (0); 10–13 (1) 14–16 (2).*

**63** *Peripetalous/semipetalous fasciole: remains independent of other fascioles (0); unites with marginal fasciole around anterior (1).*

**64** *Peripetalous fasciole and marginal fasciole: unite in interambulacral zones 1 and 4 immediately to the posterior of the anterior petals (0); unite in interambulacra 2 and 3 to the anterior of the anterior petals (1).*

**65** *In interambulacrum 4a marginal fasciole crosses on: plate 4 (0); plate 5 (1).* The marginal and peripetalous fascioles branch either on plate 4 or plate 5 in interambulacrum 4a. In forms where the marginal and peripetalous fascioles are distinct the former crosses plate 4, and this is therefore likely to be primitive.

**66** *Peripetalous band: crosses lateral interambulacral zones without indentation (0); runs vertically for one plate in interambulacral columns 1b and 4a (1); for two plates in interambulacral columns 1b and 4a (2); runs vertically for three plates in interambulacral columns 1b and 4a (3).* In spatangoids whose peripetalous fasciole unites with the marginal fasciole the peripetalous element always runs vertically through several interambulacral plates in the column immediately behind the anterior petals. This is true, even where the latero-anal portion of the marginal fasciole is absent, as in *Hypselaster*. In forms with only a peripetalous fasciole there may be little or no indentation of the fasciole, or there may be strong indentation.

**67** *Peripetalous fasciole splits anteriorly into two or more parts: no (0); yes (1).*

**68** *Fasciole runs vertically across two or more plates in interambulacral columns 2a, 3b adjacent to the frontal ambulacrum: no (0); yes, steps up one plate (1); yes, steps up two or more plates (2).*

**69** *Fasciole bounds the ends of the anterior petals: no (0); yes (1).* In some taxa the anterior petals consistently end a short but distinct distance above the fasciole (marginal/peripetalous). Scored as unknown in forms lacking petals.

**70** *Marginal/peripetalous fasciole band: crosses ambulacrum III on plates 3/4 and interambulacral zones 2 and 3 on plates 3a/b (inframarginal) (0); crosses ambulacrum III on plates 7/8 above ambitus and interambulacral zones 2b and 3a on plate 4 (1); crosses interambulacral zones 2b and 3a on plates 5 or above (2).*

**71** *Internal fasciole present: no (0); yes (1).*

**72** *Internal fasciole: divides petals in two (0); pores of paired ambulacra inside the internal fasciole rudimentary (1).*

#### 73–79. Tuberculation

**73** *Aboral tubercles: set in strong epistroma so that the tubercles appear dense and sunken (0); epistroma minimally developed so that tuberculation is superficial (1).*

**74** *Presence of primary tubercles on aboral interambulacra: no (0); yes (1).* Enlarged primary tubercles are present in some taxa scattered over the entire aboral surface, or restricted to certain interambulacral zones.

75 Primary aboral tubercles with deeply sunken areoles: no (0); yes (1). In the derived state tubercles are so deeply sunken that the test is thickened on the inner surface underneath each tubercle.

76 Primary aboral tubercles: crenulated (0); non-crenulate (1). Scored as ? where there are no primary tubercles.

77 Sternal plates: fully tuberculate (0); anterior part of sternal

plates naked but posterior half tuberculate (1); sternal plates largely naked with tubercles only at the very rear of the sternal plates (2).

78 Latero-oral tubercles enlarged and with spiral parapet (as in *Lovenia*): no (0); yes (1).

79 Enlarged tubercles bordering anterior ambulacrum: no (0); yes, as adradial band (1); yes as aligned bands forming apical tuft region (2).

Data matrix

<i>Cyclaster</i>	1 1 00010111	0010000000	1020000010	01 2 1010000	0101010021	0 001001 0 0?	1 1 0??0&10012	0?100?000
<i>Isaster</i>	1 1 00000100	2010000000	0020000010	01 2 1010000	0001010011	1 00???? ? 0?	0 ? ??? ? ????	0?100?000
<i>Isoapatagus</i>	1 1 00000000	2010000000	0020010210	01 3 1010000	0001010011	1 00???? ? 0?	0 ? ??? ? ????	0?100?000
<i>Micraster</i>	1 0 00000111	1?10000001	1020000110	01 2 1010000	0001010020	0&1001001 0 0?	0 ? ??? ? ????	0?100?000
<i>Allobrissus</i>	2 0 21000000	0010001003	1020000110	01 1 1010010	2121100010	3 001010 1 0?	1 1 0?? 1 0111	0?1000000
<i>Anabrissus</i>	2 2 20000000	0010001100	0020000010	01 1 1010010	2121100010	? 001010 1 0?	1 ? 0?? ? 0???	0?1000000
<i>Brissus</i>	2 0 21000000	0010001000	1020000110	01 1 1010010	2121100010	2 001010 1 0?	1 1 0?? 1 0111	0?1000000
<i>Cionobrissus</i>	2 0 21000111	0010001003	0020000110	01 2 1010010	2122100020	2 001010 2 0?	1 1 0??0&10111	0?1100001
<i>Hysteraster</i>	2 0 21000000	0010001000	1020000110	0? 2 10100?0	?????10010	? 001010 2 0?	1 ? 0?? 0 000?	0?1100000
<i>Plesioapatagus</i>	2 4 21000111	0010001000	1020001110	01 3 1010010	2101110010	? 001010 1 0?	1 1 0?? 0 0111	0?1100000
<i>Migliorinia</i>	1 0 21000000	0010001000	0010000210	01 2 0010010	2102121000	2 001010 2 0?	1 0 0?? 0 001?	0?100?001
<i>Meoma</i>	1 0 21000111	0010000000	1021000220	01 1 1010010	1101000020	3 001010 1 0?	1 1 0?? 1 0212	0?1000000
<i>Metalia</i>	2 0 21000111	1010101003	1021000110	01 1 1010011	2102100010	2 001010 2 11	1 1 0?? 1 0111	0?100?001
<i>Anametalia</i>	2 0 21000111	1010000003	1021000210	01 1 1010010	2102100010	3 001010 2 0?	1 1 0?? 0 0012	0?1000001
<i>Eobrissus</i>	1 0 21000000	0010100000	1021000110	01 1 1010011	2102100010	2 001010 2 11	1 1 0?? 1 0111	0?1000001
<i>Plagiobrissus</i>	1 0 21000111	0010100003	0021000110	01 1 1010011	2102100010	2&3101010 2 11	1 1 0?? 0 0111	0?1100001
<i>Rhabdobrissus</i>	1 0 21000000	0010000000	0011000110	01 1 1010010	2102100010	3 001010 2 11	1 1 0?? 0 0111	0?1100001
<i>Rhynobrissus</i>	1 0 21000000	0010001000	1020000110	01 1 1010010	2102100010	3 001010 2 10	1 1 0?? 0 0012	0?100?000
<i>Spatagobrissus</i>	1 0 21000000	0010000000	0020001111	01 2 1010010	2122010010	1 001010 2 0?	1 1 0?? 0 0012	0?100?000
<i>Archaeopneustes</i>	1 0 21000000	0000000000	0020000221	00 3 4010010	1001010020	2 00???? ? 0?	0 ? ??? ? ????	0?1100000
<i>Brissopsis</i>	1 0 21000111	1210000001	1010000010	01 1 1010010	2101100020	2 001010 1 11	1 1 0?? 1 0111	0?110?001
<i>Atelospatangus</i>	1 0 21000121	0010?00000	0000001111	01 ? ?010010	?0?211010	? 001010 1 0?	0 ? ??? ? ????	0?111?01?
<i>Eupatagus</i>	2 0 21000000	0010101003	0011001111	01 4 1010010	2102220000	2&3001010 2 0?	1 1 0?? 0 0111	0?1100001
<i>Elipneustes</i>	2 0 21000010	0010001003	0020002211	01 4 1010010	2102220100	2 001010 2 0?	1 0 0?? 0 0???	0?110?000
<i>Eurypatagus</i>	2 0 21000000	0010001003	0020000220	00 4 1010010	2102220100	3 00???? ? 0?	0 ? ??? ? ????	0?1100210
<i>Platybrissus</i>	2 0 20000000	0010000003	0010000121	00 4 1010010	2102120000	3 00?0?? 2 0?	0 ? ??? ? ????	0?100?100
<i>Granobrissoides</i>	1 0 21000000	0010000000	0011001111	01 2 1010010	2102100010	2 001010 2 0?	1 1 0??0&10111	0?100?001
<i>Goniomaretia</i>	1 1 21000000	0010100100	0010001111	01 2 1010010	2102120000	2 001010 2 0?	0 ? ??? ? ????	0?1110010
<i>Hemimaretia</i>	2 1 21000111	0010010003	00?000?110	01 2 1010010	?10?220000	? 001010 2 0?	0 ? ??? ? ????	0?101?111
<i>Lissospatangus</i>	1 0 21000000	0010101000	0020001111	01 2 ?010010	?102110000	? 001010 2 0?	1 1 0?? 0 0011	0?100?000
<i>Gymnopatagus</i>	2 0 21000121	0010000000	0020001111	01 3 1010010	2102220000	? 001010 2 0?	1 ? 0?? 0 011?	0?1100001
<i>Linopneustes</i>	1 0 21000010	0010000000	0020002211	01 3 1010010	2102220010	2 001010 2 0?	1 0 0?? 0 0101	0?1100000
<i>Maretia</i>	2 0 21000010	0010000003	0011001121	01 3 1010010	2102220000	3 001010 2 0?	0 ? ??? ? ????	0?1100100
<i>Mazzettia</i>	2 0 2?000111	0010?00000	002?0012?1	0? 3 1010010	21022200?0	? 001010 2 ??	? ? ??? ? ????	0?110?000
<i>Spatangus</i>	1 0 21000111	0010000000	0010001111	01 1 1010010	2101100010	2 0010101&20?	0 ? ??? ? ????	0?1100002
<i>Granopatagus</i>	1 0 21000121	0010000000	0010001011	01 1 1010010	2101100010	? 001010 1 0?	0 ? ??? ? ????	0?100?002
<i>Plethotaenia</i>	1 0 21000121	0010000000	0010001011	01 1 1010010	2101100010	3 001010 2 0?	1 1 0?? 0 1012	0?110?002
<i>Taimanawa</i>	1 0 21000121	0010002000	0020000010	01 1 1010010	2101100020	? 001010 1 0?	1 1 0?? 0 021?	0?1100002
<i>Schizobrissus</i>	1 0 21000121	0010002000	1021000120	01 1 1010010	1101100020	2&3001010 1 0?	1 1 0?? 1 0211	0?1100000
<i>Breyenia</i>	1 0 21000110	0010000000	0111001211	01 3 1010010	2102110000	3 001010 2 0?	1 1 0?? 0 0001	11111?002
<i>Lovenia</i>	1 0 21000110	1110100000	0110001211	012&31010010	2102120000	3 01101 0 10?	0 0 ??? ? ????	11111?112
<i>Echinocardium</i>	1 0 21000110	1121100000	0110001211	01 2 1010010	2102100010	3 00101 0 210	0 0 ??? ? ????	11100?002
<i>Paramaretia</i>	1 0 21000000	0010000000	0010000220	00 4 1010010	2101220010	2 00101 0 10?	0 ? ??? ? ????	0?111?210
<i>Gualtieria</i>	1 0 21000010	0010000000	0010001111	01 3 1010010	1101110000	3 00101 0 10?	1 0 0?? 0 0022	0?110?002
<i>Hemipatagus</i>	1 0 21000111	0010100000	0010001111	01 2 1010010	2101210000	2 00101 0 10?	0 ? ??? ? ????	0?111?111
<i>Pseudolovenia</i>	2 0 21000121	0010110003	0010000211	01 3 1010010	?10120000	? 00101 0 10?	0 ? ??? ? ????	11111?111
<i>Pycnolampas</i>	2 ? 2?000000	0010001100	00?000001?	01 3 1010010	2102120000	2 00101 0 20?	1 1 0?? 0 00??	0?100?100
<i>Paleobrissus</i>	1 3 20001000	0010011000	0020000210	01 2 1010010	2102110010	2 00101 0 20?	0 ? ??? ? ????	0?100?000
<i>Palaeotrema</i>	2 2 20001000	0000021?0?	00?00???1?	01 2 1010010	2102100000	2 00101 0 20?	0 ? ??? ? ????	0?100?001
<i>Palaeotropus</i>	1 3 20001000	0000021?0?	00?00???1?	11 1 1010010	2102100000	? 00101 0 20?	0 ? ??? ? ????	0?100?000

Continued

<i>Scrippsechinus</i>	1 0 21001000	000001000?	00?00?????	11 1 1010010	2102000010	2 00101 0 ?0?	0 ? ??? ? ????	0?100?000
<i>Archechinus</i>	2 1 21000010	0?10001000	0020000210	01 3 1010010	2101110000	2 00101 0 10?	1 1 0?? 0 001?	0?100?000
<i>Macropneustes</i>	1 0 21000111	0010000000	1020000210	01 2 1010010	2101100010	2 00101 0 10?	1 1 0?? 0 0012	0?100?000
<i>Hemiaster</i>	1 0 00000111	1?10000001	1020000110	01 3 2100000	0000110011	0 00000 0 ?0?	1 0 0?? 1 0012	0?100?000
<i>Mecaster</i>	1 0 20000111	1?20000001	1020000110	01 3 2010000	0000110110	1 00000 0 ?0?	1 0 0?? 1 0011	0?100?000
<i>Toxaster</i>	1 0 00000111	2010002002	0020002111	01 4 2100000	0000010000	1 00000 0 ?0?	0 ? ??? ? ????	0?100?000
<i>Somaliaster</i>	1 0 00000111	0?10000000	1020000210	00 4 3001000	0010000000	1 00000 0 ?0?	1 ? 0?? 0 0011	0?100?000
<i>Iraniaster</i>	1 0 00000111	0010000000	1020000210	00 3 3001100	0010000000	1 00000 0 ?0?	1 0 0?? 0 0011	0?100?000
<i>Coraster</i>	2 0 00000001	0000020?0?	00?00??1?	00 2 0010000	0020020030	0 00000 0 ?0?	1 0 0?? 1 00?1	0?200?000
<i>Homoeaster</i>	1 0 00000011	0010010001	0020010110	00 2 0010000	0000020000	1 00000 0 ?0?	1 0 0?? 0 0001	0?200?000
<i>Sphenaster</i>	2 2 ?0001100	1?10020?0?	?0?00?????	00 2 0010000	00?00200?0	0 00000 0 ?0?	1 0 0?? 0 01?1	0?100?000
<i>Aeropsis</i>	20&200001000	1210020?0?	?0?00??0?	00 2 0010000	00000200?0	0 10000 0 ?0?	10&10?? 0 00?0	0?100?000
<i>Amphipneustes</i>	1 1 20020100	1010000000	1020000211	00 3 2010000	0001110020	1 00000 0 ?0?	0 ? ??? ? ????	0?10?000
<i>Pseudabatus</i>	1 1 20020100	1010000000	1020000210	00 3 3010000	0001110020	1 00010 0 ?0?	1 0 101 2 0011	0?100?000
<i>Genicopatagus</i>	1 1 20020100	1010000000	1020000110	00 4 4010000	0001110020	1 00000 0 ?0?	0 ? ??? ? ????	0?100?000
<i>Schizocosmus</i>	1 1 20020100	1010000000	1020000111	01 3 3000000	0001010020	2 00010 0 ?0?	1 0 110 2 0001	0?100?000
<i>Parapneustes</i>	1 1 20020111	2010000000	1020000111	01 1 2010000	0001010020	2 00010 0 ?0?	1 1 100 2 0001	0?100?000
<i>Abatus</i>	1 1 20020111	1210002001	1010000111	01 1 2010000	0001100010	2 00010 0 ?0?	1 0 100 2 0011	0?100?001
<i>Tripylus</i>	1 1 20020111	1010000000	1010000111	01 1 2010000	0001100010	2 00010 0 ?0?	1 1 100 2 0001	0?100?000
<i>Sarsiaster</i>	1 3 21000100	1210001002	1010000110	01 3 2010000	001111001?	? 00000 0 ?0?	1 0 0?? 1 0012	0?100?000
<i>Paraster</i>	1 0 21100211	1220002002	1010000110	11 1 2010000	0001100010	2 00010 0 ?0?	1 1 101 2 0011	0?100?000
<i>Hypselaster</i>	1 2 20001211	1220002002	1010000110	11 2 1010000	0001100010	2 00010 0 ?0?	1 1 101 1 0011	0?100?000
<i>Ova</i>	1 2 20000211	1221002002	1010000110	01 1 3010000	0001100010	2 00010 0 ?0?	1 1 101 1 0011	0?100?000
<i>Periaster</i>	1 0 00000111	1?20000001	1010000110	01 2 1010000	0001100010	2 00010 0 ?0?	10&11011&21011	0?100?000
<i>Mundaster</i>	1 0 00000110	1?10000000	1020000110	0? 2 2010000	0001000010	1 00010 0 ?0?	1 ? 0?0 1 0011	0?100?000
<i>Lutetiaster</i>	1 0 20000111	1?10000001	1010000110	01 2 1010000	0001000010	2 00010 0 ?0?	1 1 101 2 0011	0?100?000
<i>Linthia</i>	1 0 20000122	1?10000000	1020000210	01 ? ?010010	?0?1?00020	2 00010 0 ?0?	10&11011&20011	0?100?000
<i>Caribbaster</i>	1 2 20000010	1?10000000	1020000210	01 2 1010000	0021100010	1 00010 0 ?0?	1 1 101 1 0011	0?100?000
<i>Moira</i>	1 2 20000211	1220000001	2020000210	11 1 2010000	0001100010	1 00010 0 ?0?	1 1 101 2 0011	0?100?000
<i>Protenaster</i>	2 0 20000111	1210001000	1020000220	01 1 3010010	0011000010	1 00010 0 ?0?	1 1 101 2 0011	0?100?000
<i>Prenaster</i>	2 0 20000000	0000001000	1020000210	01 1 ?010000	0001100010	2 00010 0 ?0?	1 1 100 2 0000	0?100?000
<i>Brisaster</i>	0 1 20010221	1220002002	1010000110	01 1 1010000	0000100020	2 00010 0 ?0?	1 1 101 2 0011	0?100?001
<i>Tripylaster</i>	1 1 21010221	1210000001	1010000110	01 1 2010000	0001100020	2 00010 0 ?0?	1 1 101 2 00?1	0?100?000
<i>Agassizia</i>	1 0 21000000	1110000002	0000000210	01 1 0010000	0001000010	1 00010 0 ?0?	1 0 100 2 0000	0?100?000
<i>Faorina</i>	1 1 20000111	1210000001	1021000110	01 2 1010010	2011000010	1 00010 0 ?0?	1 1 0?? 1 101?	0?100?000
<i>Plesiozonus</i>	1 1 20000001	0010000000	0021002210	00 2 1010010	1011000010	1 00010 0 ?0?	1 1 0?0 0 0011	0?100?000
<i>Paleopneustes</i>	1 1 20000000	00100100?0	0021002110	00 3 2010010	2011000020	2 00010 0 ?0?	1 1 0?00&10011	0?10?000
<i>Pericosmus</i>	1 1 20000111	1010000000	1021000110	01 2 1010010	0001000010	2 00010 0 ?0?	1 1 0?0 2 0011	0?100?000